Development of Epigenetic Modifiers with Therapeutic Potential in FMS-Related Tyrosine Kinase 3/Internal Tandem Duplication (FLT3/ITD) Acute Myeloid Leukemia and Other Blood Malignancies

Development of Epigenetic Modifiers with Therapeutic Potential in Fms-related tyrosine Kinase 3 / Internal Tandem Duplication (FLT3/ITD) Acute Myeloid Leukemia and other Blood Malignancies

Gabriele Carullo[1,#], Sara Rossi[1,#], Valentina Giudice[2], Alex Pezzotta[3], Ugo Chianese[4], Pasqualina Scala[2], Sabrina Carbone[3], Anna Fontana[1], Giovanna Panzeca[1], Silvia Pasquini[5], Chiara Contri[6], Sandra Gemma[1,*], Anna Ramunno[7], Simona Saponara[8], Francesca Galvani[9], Alessio Lodola[9], Marco Mor[9], Rosaria Benedetti[4,10], Carmine Selleri[2], Katia Varani[6], Stefania Butini[1], Lucia Altucci[4,10,11], Fabrizio Vincenzi[6], Anna Pistocchi[3], Giuseppe Campiani[1,12,*]

[1]Department of Biotechnology, Chemistry and Pharmacy, University of Siena, Via Aldo Moro 2, 53100 Siena, Italy
[2]Department of Medicine, Surgery, Dentistry “Scuola Medica Salernitana”, University of Salerno, Via S. Allende, 84081 Baronissi (SA), Italy
[3]Department of Medical Biotechnology and Translational Medicine, University of Milan, LITA, Via Fratelli Cervi 93, 20054, Segrate (MI), Italy
[4]Department of Precision Medicine, University of Campania Luigi Vanvitelli, Via de Crecchio 7, 80138 Naples, Italy.
[5]Department of Chemical, Pharmaceutical and Agricultural Sciences, University of Ferrara, Via Borsari 46 44121 Ferrara, Italy
[6]Department of Translational Medicine, University of Ferrara, Via Borsari 46 44121, Ferrara, Italy.
[7]Department of Pharmacy, University of Salerno, Via Giovanni Paolo II, 132, 84084, Fisciano (SA), Italy.
[8]Department of Life Sciences, University of Siena, Via Aldo Moro 2, 53100 Siena, Italy.
[9]Department of Food and Drug, University of Parma, Parco Area delle Scienze 27/A, 43124, Parma, Italy.
[10]Program of Medical Epigenetics, Vanvitelli Hospital, Naples, Italy.
[11]Biogem Institute of Molecular and Genetic Biology, 83031, Ariano Irpino, Italy.
[12]Bioinformatics Research Center, School of Pharmacy and Pharmaceutical Sciences, Isfahan University of Medical Sciences, Isfahan 81746-7346, Iran.

Abstract

Blood cancers encompass a group of diseases affecting blood, bone marrow or the lymphatic system, representing the fourth most commonly diagnosed cancer. Leukemias are characterized by a dysregulated proliferation of myeloid and lymphoid cells, with different rates of progression (acute or chronic). Among the chronic forms, hairy cell leukemia (HCL) is a rare disease and no drugs have been approved to date. On the other hand, acute myeloid leukemia (AML) is one of the most aggressive malignancies, with a low degree of survival especially in the case of FLT3-ITD mutations. Epigenetic modifications emerged as promising strategies for the treatment of blood cancers. Epigenetic modulators such as histone deacetylase (HDAC) inhibitors are increasingly used for targeted cancer therapy. New hydroxamic acid derivatives, preferentially inhibiting HDAC6 (**5a**-**q**), were developed and their efficacy was investigated in different blood cancers, including multiple myeloma (MM), HCL and AML, pointing out their pro-apoptotic effect as the mechanism of cell death. Among the inhibitors here described, **5c**, **5g** and **5h** were able to rescue the hematopoietic phenotype *in vivo* using the FLT3-ITD zebrafish model of AML. **5c** (*leuxinostat*) proved its efficacy also in cells from FLT3-ITD AML patients promoting a marked acetylation of α-tubulin compared to histone H3, confirming HDAC6 as a preferential target for this new class of hydroxamic acid derivatives at the tested doses.

Keywords: hairy cell leukemia, acute myeloid leukemia, HDAC inhibitors, FLT3, apoptosis, zebrafish, HDAC6

List of Abbreviations

ALL, acute lymphocytic leukemia; AML, acute myeloid leukemia; CHT, caudal hematopoietic tissue; CLL, chronic lymphocytic leukemia; CML, chronic myeloid leukemia; CPP, coronary perfusion pressure; DCM, dichloromethane; ECG, electrocardiogram; ERG, electroretinogram; EtOAc, ethyl acetate; EtOH, ethanol; FLT3, FMS-like tyrosine kinase 3; H_2O, water; HCL, hairy cell leukemia; HDAC, histone deacetylase; HR, frequency; HSPCs, hematopoietic stem and progenitor cells; ITD, internal tandem duplications; KOH, potassium hydroxide; LVP, left ventricular pressure; PBMCs, peripheral blood mononuclear cells; PQ, atrioventricular conduction time; pTSA: *p*-toluenesulfonic acid; QRS, intraventricular conduction time; QTc, corrected QT (action potential duration); RR, cycle length; TEA, triethylamine; TFA, trifluoroacetic acid; TKD, tyrosine kinase domain; ZBG, zinc binding group.

Blood cancers (BCs) encompass a heterogeneous group of hematological malignancies, affecting peripheral blood, bone marrow, or the lymphatic system. BCs have a high incidence with 14-19 new cases per 100,000 population in Western Countries, accounting for around 9% of all cases of cancers and represent the fourth most diagnosed cancer with a growing trend in the last decades.[1,2]

Leukemias and lymphomas comprehend a plethora of malignancies characterized by uncontrolled proliferation of cells originating from myeloid and lymphoid lineages.[3] Prognosis varies based on disease aggressiveness related to clinical presentation, phenotypic and molecular signatures, typically resulting in poor survival rates for adult acute leukemias, or in more favorable outcomes for indolent lymphomas.[4]

Leukemias are primarily classified based on progression rate (acute or chronic) and the specific blood cell lineages affected (myeloid or lymphoid), including acute lymphocytic leukemia (ALL), chronic lymphocytic leukemia (CLL), acute myeloid leukemia (AML), and chronic myeloid leukemia (CML).[5]

CLL is the most common type of leukemia in the elderly and is associated with the accumulation of $CD5^+$ B cells in peripheral blood and lymphoid organs.[6] Conversely, hairy cell leukemia (HCL), a rare chronic B-cell lymphoma deriving from late-activated post-germinal memory B-cells, is characterized by the presence of medium-sized mature $CD5^-$ lymphocytes with “hairy” projections in the bone marrow, spleen, and less frequently lymph nodes.[7] Classical CLL and HCL can harbor somatic mutations in tumor protein 53 (*TP53*), with various frequencies, ranging from 0 to 27%.[8] To date, there are no curative treatments for these clinical manifestations, as HCL patients are treated with cladribine-based regimens as first-line therapy, although the use of BRAF inhibitor vemurafenib in association with anti-CD19 monoclonal antibodies for the treatment of relapse/refractory HCL patients has been attempted.[9]

Moreover, inactivating coding variants of epigenetic enzymes have been identified in B cells from HCL patients, suggesting that these enzymes could have a potential therapeutic role in disease recurrence.[10] Recurrence and high relapse rates point out the urgency of new treatments.[11]

Among acute malignancies, AML is an aggressive BC with extremely poor 5-year survival and a high relapse rate, especially in those subjects who fail to achieve complete remission after induction therapy.[12] AML is characterized by differentiation block and accumulation within the bone marrow of immature myeloid progenitor cells,[13] that can harbor several genetic abnormalities favoring cell proliferation and survival, such as those in FMS-like tyrosine kinase 3 (FLT3) and *TP53*.[14]

Specifically, one-third of AML patients have different FLT3 mutations: *i)* FLT3-TKD, a missense point mutation in a highly conserved region, i.e. the activation loop of the tyrosine kinase domain (TKD), found in approximately 7% of AML patients; *ii)* FLT3-ITD, internal tandem duplications (ITDs) of the juxtamembrane domain, found in 25% of AML patients. Patients with FLT3-ITD are classified as intermediate-risk AML, according to 2022 European LeukemiaNet risk stratification system, and can specifically benefit from the use of FLT3 inhibitor (FLT3i) gilteritinib as monotherapy in relapsed/refractory AML[15] or as maintenance therapy[16] after hematopoietic stem cell transplantation.[17,18] Therefore, mutational screening during the diagnostic process is crucial for an accurate assessment of disease prognosis. However, inhibitor-resistant FLT3 mutations can arise[19] by on- or off-target mechanisms, often recruiting downstream pathways like JAK/STAT and PI3K/Akt, with a consequent decrease in FLT3i efficacy.[20]

Combination therapies have been attempted to overcome resistance with scarce efficacy and unpredictable drug−drug interactions causing cumulative toxicity.[19] In addition, FLT3 mutated cells could be eradicated by potentiating proteasomal or lysosomal degradation pathways, and by indirect mechanisms, conceivably mediated by epigenetic modifiers.[21]

HDAC inhibition in blood malignancies could afford sufficient therapeutic windows to achieve durable remissions by reversing cancer-associated epigenetic states. Noteworthy, AML cells show dysregulated HDAC activity and overexpress HDAC6.[22] Hence, in FLT3-ITD AML, HDAC inhibition decrease leukemic stem cell expansion[23] and may induce the degradation of FLT3-ITD by disrupting the HDAC6/Hsp90/FLT3-ITD axis.[24]

HDAC enzymes are categorized into four major families, based on their similarity, cellular localization, and enzymatic activities. Class I nuclear enzymes is represented by HDAC1, 2, 3, and 8. Class II is split into two subfamilies: IIa which includes HDAC4, 5, 7, and 9; IIb which comprises HDAC6 and 10. Class IV includes only HDAC11. All enzymes are zinc-dependent, except for Class III HDACs that possess NAD-dependent catalytic sites, consisting of seven proteins of the sirtuins family (SIRT 1-7).[25,26]

Non-selective HDAC inhibitors (HDACis), like FK228 and panobinostat (**1**, **Figure 1**), induce proteasomal degradation of FLT3-ITD without FLT3i- associated relapse.[27,28] The Food and Drug Administration has approved HDACis for myeloma and lymphoma (**1** and **SAHA 2**, respectively, **Figure 1**). Due to toxicity issues,[29] *pan*-HDACis have not been approved yet for AML (also FLT3 mutated) or HCL (only combinations of cladribine and **SAHA**/entinostat have been investigated with limited efficacy[30]). Indeed, non-selective HDACi tolerability needs to be considered, especially in older and frail or pediatric patients.[31]

Specifically, side effects are generally associated with *pan*-HDAC inhibition in therapy, which could be, in turn, limited by targeting preferentially relevant isoforms in leukemic cells. HDAC5, 6 and 9 are overexpressed in AML tissues, while HDAC9 in HCL;[22] however, the physiopathological role of HDAC5 and HDAC9 is still under debate.[32]

Recently, HDAC6 inhibition has been proven to be correlated to a reduced expansion of leukemic cells *in vitro* and *in vivo*, highlighting the possibility of lowering FLT3-ITD primitive leukemia cells without interfering with the physiological activity of FLT3 kinase.[23]

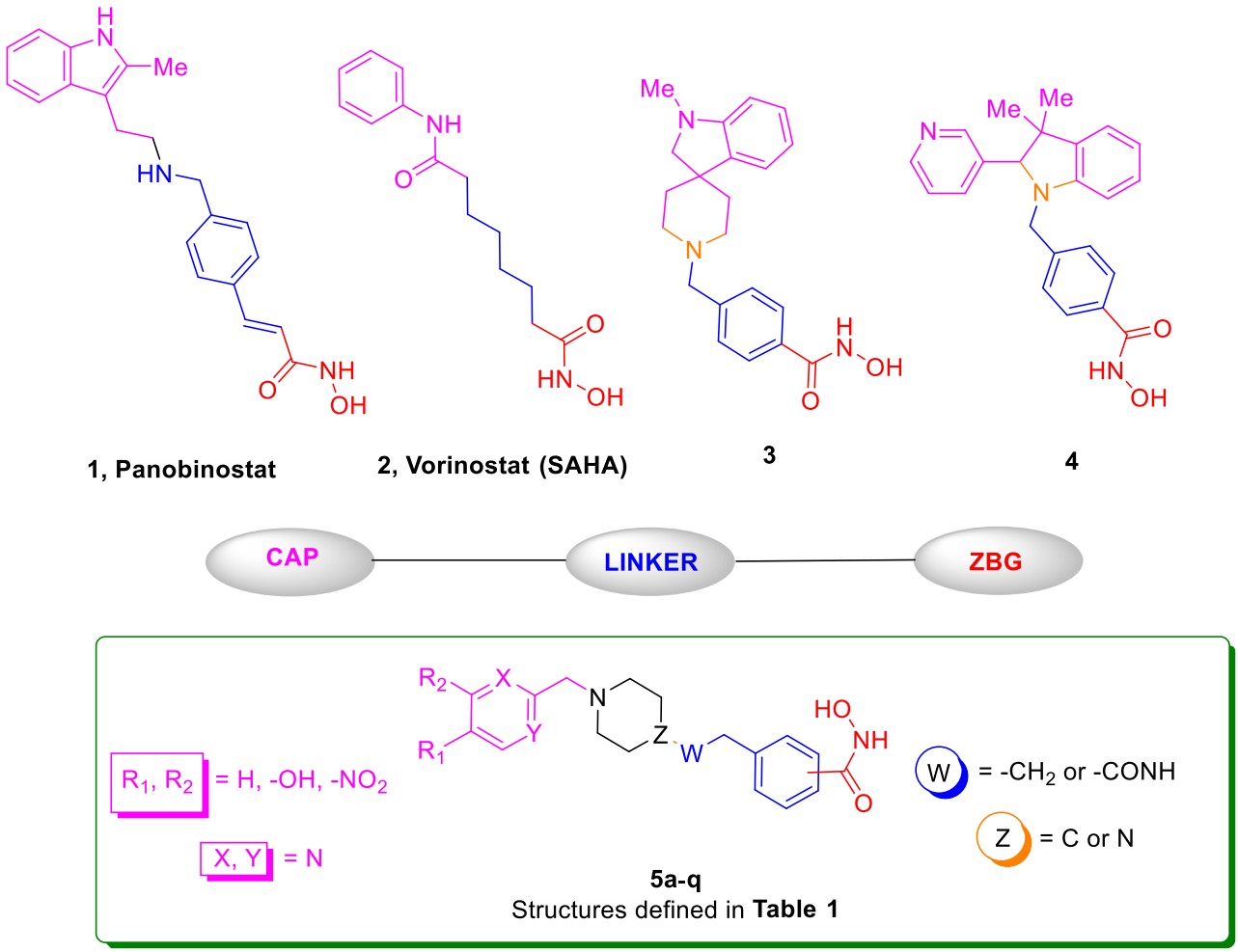

Figure 1. Known HDAC inhibitors and general structure of title compounds **5a-q**.

In the absence of approved drugs that confer tumor control in HCL and FLT3-ITD AML, there is urgency to identify new therapeutic tools to specifically eradicate the diseases. Zebrafish has emerged as a fascinating animal model for understanding the pathogenesis of human diseases and has proven to be a versatile and reliable *in vivo* experimental model to study hematological malignancies[33] and to identify potential therapeutic tools.[23] Based on our previous experience in HDACi development,[34,35] we designed a series of novel HDAC inhibitors (**5a-q**, **Figure 1** and **Table 1**), characterized by specific

physicochemical properties, efficacious in MM and different leukemias, for *in vivo* testing in a zebrafish AML model.

Herein, we report new HDACis (**5a**-**q**, **Figure 1** and **Table 1**) preferentially targeting HDAC6, possessing a surface recognition group (CAP), a zinc-binding group (ZBG), and a connecting unit (LINKER).

5a-**q** were designed exploiting the X-ray structure (PDB 6V7A) of compound **3**[36] (**Figure 1**) in complex with *zf*HDAC6 with the help of computer simulations and considering the effect of specific structural features of **4** in blocking HDAC6 enzyme (**Figure 1**).[34]

A green synthetic approach was applied to obtain both amine (**5a**-**f**) and urea derivatives (**5g**-**q**), tested on a panel of HDAC isoforms. To evaluate target engagement and anticancer profile, selected compounds were tested in cell-based assays using THP1 (peripheral blood acute monocytic leukemia), K562 (chronic myeloid leukemia, CML), U937 (pro-monocytic histiocytic lymphoma), MEK1 (CLL), MOLT-4 (acute lymphoblastic leukemia) and NB4 (acute promyelocytic leukemia) cells, demonstrating induction of apoptosis as the mechanism of cell death.

Moreover, a FLT3-ITD AML zebrafish model was employed for determining *in vivo* efficacy of compounds in terms of reduction of the hematopoietic stem cell expansion driven by the FLT3-ITD mutation, while HDACi-induced cell death mechanisms were studied in *ex vivo* FLT3-ITD AML cells and *in vitro* MM and HCL tumors.

Table 1. Inhibitory activity of compounds **5a**-**q** toward *h*HDAC6, *h*HDAC1, *h*HDAC10, HDAC3, HDAC5, HDAC8 and *h*HDAC11 (as IC_{50}, nM).

Cpd		IC_{50} (nM) *h*HDAC6	*h*HDAC1	*h*HDAC10	*h*HDAC8	*h*HDAC3	*h*HDAC5	*h*HDAC11
5a	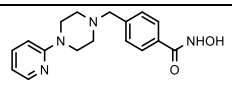	346 ± 24	NT[a]	NT[a]	NT[a]	NT[a]	NT[a]	NT[a]
5b	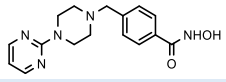	322 ± 21	NT[a]	NT[a]	NT[a]	NT[a]	NT[a]	NT[a]
5c	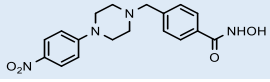	30 ± 2	1203 ± 87	4811 ± 302	2446 ± 165	2858 ± 153	>10000 (17%)	5570 ± 358

5d	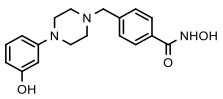	104 ± 7	>10000 (42%)	>10000 (38%)	NT[a]	NT[a]	NT[a]	NT[a]
5e	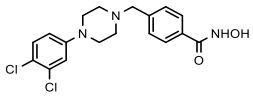	970 ± 68	NT[a]	NT[a]	NT[a]	NT[a]	NT[a]	NT[a]
5f	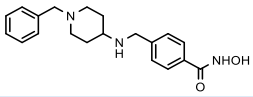	>10000 (43%)	NT[a]	NT[a]	NT[a]	NT[a] -	NT[a]	NT[a]
5g	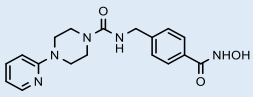	75 ± 6	2374 ± 148	3975 ± 211	3187 ± 214	1369 ± 93	>10000 (3%)	5372 ± 308
5h	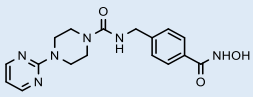	56 ± 4	4799 ± 273	5383 ± 332	5692 ± 339	1447 ± 87	>10000 (15%)	3162 ± 221
5i	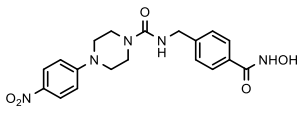	73 ± 5	4678 ± 294	5385 ± 284	NT[a]	NT[a]	NT[a]	NT[a]
5j	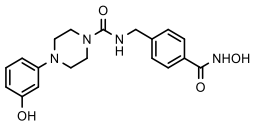	78 ± 6	5740 ± 378	2504 ± 146	7293 ± 480	NT[a]	NT[a]	NT[a]
5k	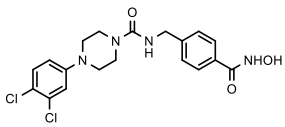	89 ± 7	639 ± 44	4448 ± 282	4425 ± 308	NT[a]	NT[a]	NT[a]
5l	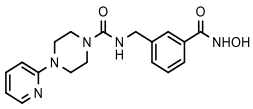	5793 ± 342	NT[a]	NT[a]	NT[a]	NT[a]	NT[a]	NT[a]
5m	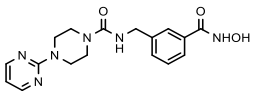	2689 ± 177	>10000 (22%)	>10000 (17%)	> 10000	NT[a]	NT[a]	NT[a]
5n	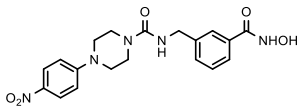	2197 ± 174	NT[a]	NT[a]	NT[a]	NT[a]	NT[a]	NT[a]
5o	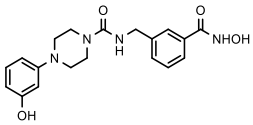	2822 ± 204	NT[a]	NT[a]	NT[a]	NT[a]	NT[a]	NT[a]
5p	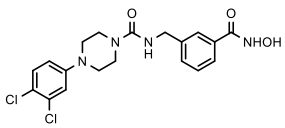	3091 ± 221	NT[a]	NT[a]	NT[a]	NT[a]	NT[a]	NT[a]
5q	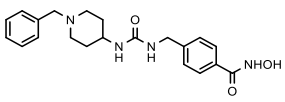	>10000 (30%)	NT[a]	NT[a]	NT[a]	NT[a]	NT[a]	NT[a]
	4	40.8 ± 1.51	5421 ± 268	NT[a]	2204 ± 198	5871 ± 376	>10000 (14%)	695 ± 41
	Panobinostat	9.55 ± 0.67	63 ± 4	6.38 ± 0.47	NT[a]	NT[a]	NT[a]	NT[a]
	Tubastatin A (TUB)	31.0 ± 2.0	1940 ± 380	NT[a]	712 ± 94	NT[a]	NT[a]	NT[a]

Each value is the mean of at least three determinations; results are expressed with ± standard error of the mean (SEM); [a]NT: not tested.

Results and Discussion

Chemistry

The target compounds **5a-q** were synthesized as reported in **Scheme 1**.

Scheme 1. Synthesis of compounds **5a-e, 5g-p** and **5f,q**[a]

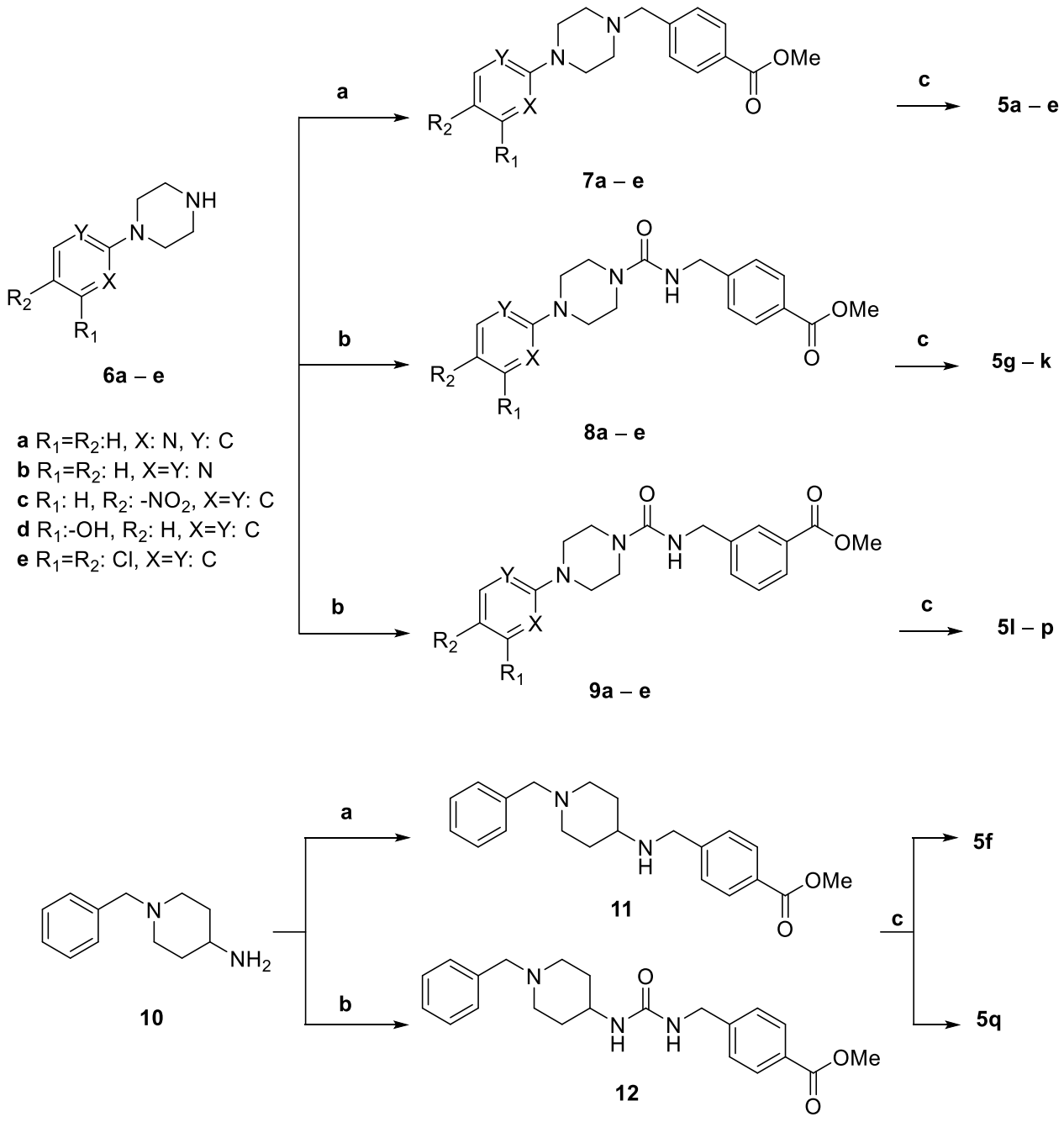

[a]Reagents and conditions: **a)** methyl 4-formylbenzoate, pTSA, EtOH, 25 °C, 24 h, then $NaBH_3CN$, 25 °C, 2 h (51–73%); **b)** methyl 4-(isocyanatomethyl)benzoate (for **8a-e, 12**), methyl 3-(isocyanatomethyl)benzoate (for **9a-e**), cyrene™, N_2, 25 °C, 6 h (50-80%); **c)** hydroxylamine hydrochloride, methanolic KOH, MeOH, 25 °C, 12 h (24-85%).

A simple protocol was set up for the synthesis of **5a-q** starting from commercially available aryl-piperazines namely 1-(pyridin-2-yl)piperazine (**6a**), 2-(piperazin-1-yl)pyrimidine (**6b**), 1-(4-nitrophenyl)piperazine (**6c**), 3-(piperazin-1-yl)phenol (**6d**), 1-(3,4-dichlorophenyl)piperazine (**6e**). In particular, **6a-e** were converted into derivatives **7a-e** under reductive amination conditions in the presence of the acid catalyst *p*-toluenesulfonic acid (pTSA)[38] and EtOH as a solvent. For the synthesis of the ureas **8a-e**, the secondary amines **6a-e** were treated with methyl 4-(isocyanatomethyl)benzoate in cyrene™, a biodegradable aprotic dipolar solvent derived from cellulose biomass. **6a-e** were converted into ureas **9a-e** by reaction with 3-(isocyanatomethyl)benzoate under the above-described conditions. For the synthesis of final compounds **5a-e** and **5g-p**, intermediates **7a-e**, **8a-e** and **9a-e** were treated with hydroxylamine hydrochloride under basic conditions.

For the synthesis of compounds **5f** and **5q**, 1-benzylpiperidin-4-amine (**10**) was treated with methyl 4-formylbenzoate in reductive amination conditions to obtain amine **11**. When **10** was exposed to methyl 4-(isocyanatomethyl)benzoate as described before,[37] urea **12** was obtained. Ultimately, **11** and **12** were converted into the final compounds **5f,q** after treatment with hydroxylamine hydrochloride under basic conditions(**Scheme 1**).

Structure activity relationships (SARs), *in vitro* HDAC inhibition and molecular modelling studies

The aim of this work was the identification of new small molecular entities preferentially inhibiting HDAC6. Analogues **5a-q** were exposed to enzymatic studies on a panel of selected HDAC isozymes, with particular attention versus HDAC6, including HDAC1, HDAC8 and HDAC10 as primary off-targets. Because of key similarities in the active sites of HDAC6 and HDAC8, discrimination between these two isoforms could be challenging. We also evaluated the activity against HDAC3, HDAC5, and HDAC11 for selected

compounds and data were compared to those of reference **4** (**Table 1**). Our SAR investigation started with the modification of the CAP fragment of our reference spiroindoline-based inhibitor **3**, recently co-crystallized within the *zf*HDAC6 binding site.[36] New compounds were designed in the attempt to form polar interactions with Ser531, as engaging interaction with this residue could improve selectivity for HDAC6.[39] In fact, this serine has been reported to form crucial hydrogen bonds with HDAC6is, either acting as a donor[40] or as an acceptor.[41]

The 1-methylspiro[indoline-3,4'-piperidine] moiety of **3** was modified into a more polar and flexible 1-(pyridin-2-yl)piperazine fragment. Docking simulations (see SI for details) showed that the resulting compound **5a** well fitted the active site of HDAC6 with its hydroxamic acid group able to chelate the zinc atom and its tail able to undertake favorable interactions with amino acids at the binding site opening. In particular, the protonated piperazine nitrogen closer to the benzoyl hydroxamic moiety formed a polar interaction with the side chain of Ser531 (**Figure 2A**), consistently with what had been reported for similar compounds.

With an IC_{50} value of 346 nM (**Table 1**), in line with the potency reported for hit **3**,[36] compound **5a** emerged as a fair hit for the present investigation. In fact, similar structures with a phenyl ring replacing the pyridine one had been described in a patent dedicated to HDAC6 inhibitors.[42] The introduction of an additional nitrogen atom into **5a** led to the 2-(piperazin-1-yl)pyrimidine derivative **5b** with no significant gain in the inhibitory potency (HDAC6 IC_{50} = 322 nM, **Table 1**). Conversely, the replacement of the pyridin-2-yl substituent with a *p*-nitrophenyl system at the nitrogen atom of the piperazine ring gave **5c** (*leuxinostat*), displaying an IC_{50} value of 30 nM toward HDAC6 and a good selectivity profile over HDAC1 (IC_{50} =1203 nM), HDAC3 (IC_{50} = 2858 nM), HDAC5 (IC_{50} > 10000 nM), HDAC8 (IC_{50} = 2446 nM), HDAC10 (IC_{50} = 4811 nM) and HDAC11 (IC_{50} = 5570 nM) (**Table 1**).

Docking pose of **5c** in complex with HDAC6 revealed the formation of an electrostatic interaction between the nitro group of **5c** and the basic side chain of Arg636 (**Figure 2B**). This polar interaction, never described in previous works, led to a 10-fold improvement in the IC_{50} value with respect to **5a**. In a similar direction, the insertion of *m*-hydroxyphenyl ring (**5d**) resulted in an IC_{50} value of 104 nM (**Table 1**), as hinted by the presence of an additional H-bond interaction between the -OH group and the -CO group of Asn645 side chain (**Figure 2C**). Conversely, juxtaposition on the 2-(piperazin-1-yl) nucleus with a 3,4-dichlorophenyl ring, resembling the *p*-chloro derivative reported in a patent,[42] was not tolerated, leading to an IC_{50} value of approximately 1 μM (**5e**, **Figure 2C** and **Table 1**). Also, a significant drop in the inhibitory potency was observed when 1-(pyridin-2-yl)piperazine moiety of **5a** was replaced by the 1-benzylpiperidin-4-amine of **5f**, which failed in inhibiting HDAC6 also in the low micromolar range (**Table 1**).

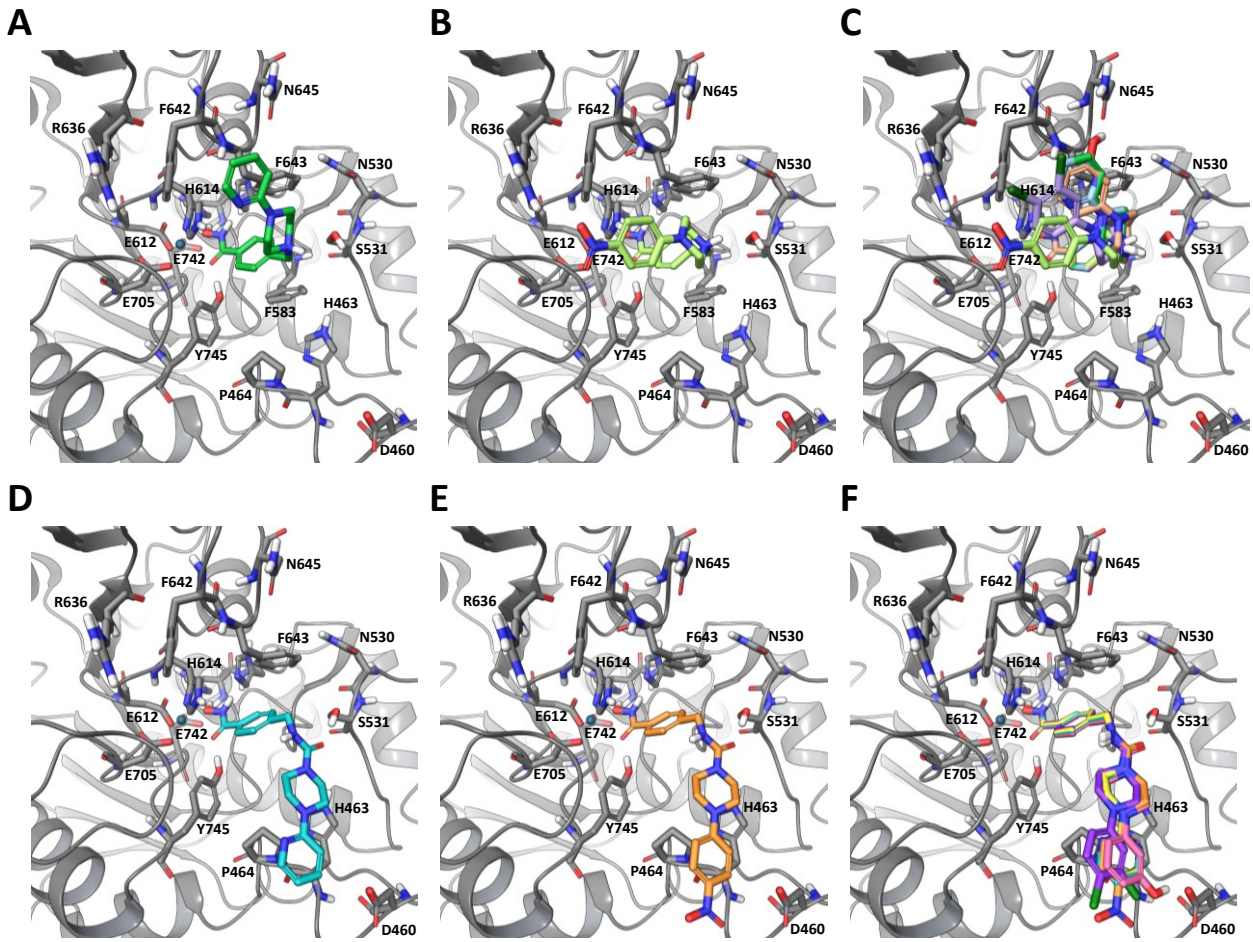

Figure 2. Best docking pose for compounds **5a** (panel A, green carbon atoms), **5c** (panel B, light green carbon atoms), **5g** (panel D, cyan carbon atoms), and **5i** (panel E, orange carbon atoms) within HDAC6 binding site (gray carbon atoms and gray cartoons). HDAC6 residues in proximity of the inhibitors and involved in Zn^{2+} (dark cyan sphere) chelation are also displayed. Panel C reports the superposition of the best docking pose for compounds **5a** (green), **5b** (light blue), **5c** (light green), **5d** (light orange), and **5e** (violet) within HDAC6 binding site (gray carbon atoms and gray cartoons). Panel F displays the superposition of the best docking pose for compounds **5g** (cyan), **5h** (yellow), **5i** (orange), **5j** (pink), and **5k** (purple) within HDAC6 binding site (gray carbon atoms and gray cartoons).

Inclusion of the basic nitrogen atom of the 1-(pyridin-2-yl)piperazine moiety of **5a** into a non-ionizable urea group, similar to what had been implemented in a different class of inhibitors, reported in a recent patent application,[43] led to the 4-(pyridin-2-yl)piperazine-1-carboxamide derivative **5g**, which showed a 5-fold improvement in the IC_{50} value (HDAC6 IC_{50} = 75 nM, **Table 1**).

This can be explained by a docking model of **5g** into the Zn^{2+} binding site of HDAC6, which showed that an alternative polar interaction with opposite polarity could be taken by the neutral carbonyl of the urea group with the side chain of Ser531 (**Figure 2D**).

A series of **5g-**analogs, in which the pyridine was replaced by a pyrimidine (**5h**), a *p*-nitrophenyl (**5i,** displayed in **Figure 2E**), a *m*-hydroxyphenyl (**5j**) or a 3,4-dichlorophenyl ring (**5k**) showed inhibition of HDAC6 with similar potency and selectivity over the panel of tested enzymes. **5g** and **5h** were tested on 7 isoforms and showed a good selectivity for HDAC6 compared to other enzymes, similarly to **5c**. Docking of these compounds into the HDAC6 binding site showed that the alternative H-bond interaction taken by the urea group induces a different orientation of the terminal aromatic group, which no longer points toward Arg636 nor Asn645, but interacts with the solvent bulk (**Figure 2F**). Thus, the effective polar interaction of the urea group guarantees good inhibitory potency to all these compounds and allowed to procced to further studies compounds **5g**, **5h**, **5j** and **5k**, avoiding the nitrophenyl group of **5c**, which may be subject to metabolic reactions with the production of potentially toxic metabolites. Thus, detailed SAR exploration of this class of

HDAC6 inhibitors allowed the identification of several derivatives with a range of different physicochemical properties and metabolic liabilities.

Finally change from *para* to *meta* position of the hydroxamic acid group (**5l**–**5p**) had a detrimental impact on inhibitory potency, showing that an efficient Zn^{2+} chelation can be achieved when the ZBG is placed at the *para* position of the phenyl ring. Finally, also the urea analogue of **5f**, namely **5q**, failed in inhibiting HDAC6.

Viability assays and target engagement in cells

Based on IC_{50} values versus HDAC6 and different selectivity profiles versus class I HDAC1, HDAC3 and HDAC8 members and class IIB member HDAC10 (**Table 1**), we selected compounds **5c**, **5g**, **5h**, **5j**, **5k** and **5m** as the most suitable to correlate biochemical inhibition with cellular potency and anticancer profile. Cellular experiments have been performed by using also known HDACis like **SAHA** (**2**), Tubastatin A (**TUB**) and PCI34051 (**PCI**) for comparison in different blood cancer cells. HDAC expression patterns in blood malignancies are heterogeneous, implying that the role of HDACs in leukemia may be related to global expression and specific expression patterns.[22] In line with this, we selected different blood lineages including THP1, K562, U937 and MEK1 cells (**Figure 3**). The selected cell lines are dissimilar regarding both the stage of differentiation as well as the hematopoietic lineage that was interrupted by the illness.[44] Moreover, the cell lines differ one another in HDAC isozyme expression and differ also in the HDAC relevance in the specific disease.[22] Noteworthy, HDAC6 is rarely expressed in primary lymphoma, and shreds of evidence demonstrated its irrelevance as a therapeutic target in these lymphoid malignancies.[45] Besides, acute leukemia cells NB4 and MOLT-4 showed increased levels of acetylated α-tubulin (non-histone substrate of HDAC6) compared to histone H3 (class I HDACs histone substrate) after a prolonged exposure to HDACis, while CLL MEK-1 cells

showed increased levels of acetyl histone H3, rendering this blood cancer highly responsive to class I (nuclear) HDACis.[46]

On the other hand, CML K562 cells displayed an initial higher acetylated α-tubulin level which decreases after prolonged incubation, questioning the efficacy of HDACis in these blood cancer types.[47] **5c**, **5g**, **5h**, **5j**, **5k**, and **5m** target engagement was evaluated through western blot analysis measuring acetylation of relevant histone and non-histone proteins for HDAC1/HDAC3, HDAC6 and HDAC8 (acetyl histone H3/K9-K14, acetyl α-tubulin and acetyl-SMC3, respectively). The effects on cell viability were interrogated at increasing concentrations (1, 10, and 50 μM) up to 72 h of incubation, in comparison to reference HDACis. As shown in **Figure 3**, the most interesting compounds proved to be **5c**, **5g**, **5h**, and **5k** which showed a dose-dependent cytotoxic effect in cancer cells when compared with **TUB** and **PCI**, while **SAHA** showed a better antiproliferative effect, confirming that its *pan*-HDAC inhibitory activity is responsible of the strong decrease in cell viability.

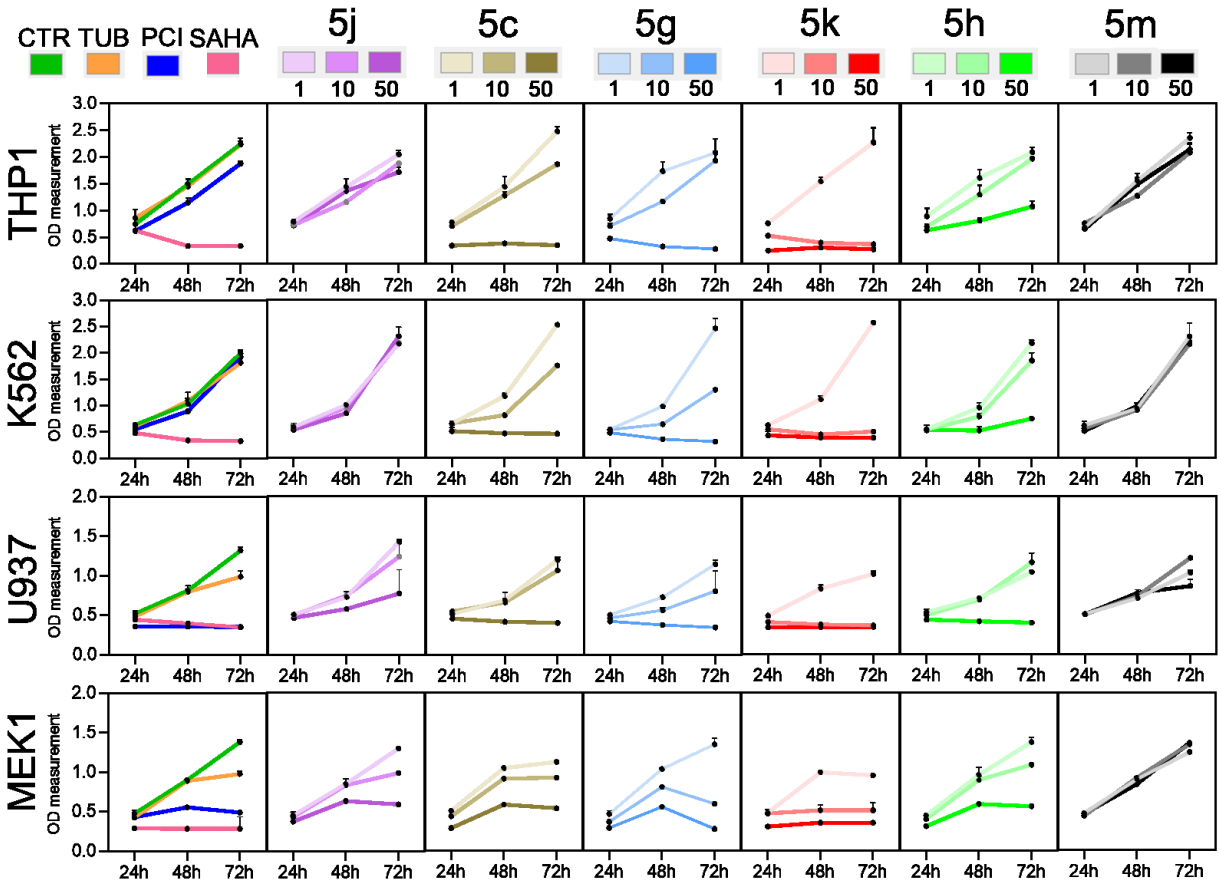

Figure 3. Proliferation assay in THP1, K562, U937, and MEK1 cell lines on a time course of 24 , 48, and 72 h. **5c**, **5g**, **5h**, **5k**, **5j**, **5m** were tested at 1, 10, 50 μM and compared to CTR, TUB (10 μM), PCI (10 μM) and SAHA (5 μM).

Of note, compound **5c**, with a low selectivity profile ($SI_{HDAC6/HDAC1}$ = 40) showed a comparable activity with the dual inhibitor **5k** ($SI_{HDAC6/HDAC1}$ = 7) (**Table 1**).

The HDAC6is **5g** and **5h** displayed high cytotoxicity only at 10 and 50 μM. The inhibitor **5j**, although presenting a nM inhibition potency versus HDAC6, showed a limited antiproliferative effect on the cancer cells of the panel (**Figure 3**).

Interestingly, the *m*-substituted analogue **5m** (displaying a micromolar inhibition potency versus HDAC6, **Table 1**) did not promote an appreciable dropdown in cell viability also at high concentrations (**Figure 3**). Furthermore, all the compounds showed limited cytotoxicity in MEK1 cells, except for compound **5k** at 50 μM. To investigate the target engagement, **5c**, **5g**, **5h**, **5k** and **5m** were examined for their ability to induce acetylation of

α-tubulin (substrate of HDAC6), histone H3 (substrate of HDAC1/HDAC3) and SMC3 (substrate of HDAC8) (**Figure 4**).

Cells were subjected to 24 h incubation with 10 μM of all the new compounds, including reference **TUB** and **PCI**, while **SAHA** was used at 5 μM.

Target engagement was analyzed *via* western blotting assays.

A significant acetylation of α-tubulin was observed in THP1 cells for all the compounds while only **5k** (and **SAHA**, **Figure 1**) was able to induce acetylation of histone H3 (**Figure 4A**), due to its potency against HDAC1 (**5k**, $IC_{50HDAC1}$ = 639 nM, **Table 1**).

Among the molecules of the panel only **PCI** was able to promote acetylation of SMC3, due to its specificity for HDAC8. **Figure 4B** pointed out that U937 cells were responsive to HDAC inhibition, with a comparable profile with that observed in THP1 cells (**Figure 4A**), highlighting the overexpression of these enzymes in myelocytic tissues. When K562 cells were analyzed for their ability to induce acetylation of histone and non-histone substrates (**Figure 4C**), a slight acetylation profile was observed. Also in this case, **5c**, **5g-h**, **5k** induced a marked acetylation of α-tubulin, with **5k** being able to markedly increase both the acetylation levels of α-tubulin and histone H3. Finally, MEK1 cells (**Figure 4D**) seem to be less responsive to the most potent HDAC6i **5c**, while compounds **5h** and **5k** were able to promote acetylation of α-tubulin and SMC3. As shown in **Figure 4A-D**, **5m** at the tested doses was not able to induce acetylation of α-tubulin presenting, although not statistically significant, only a slight acetylation of histone H3, in all the tested blood cancer cells.

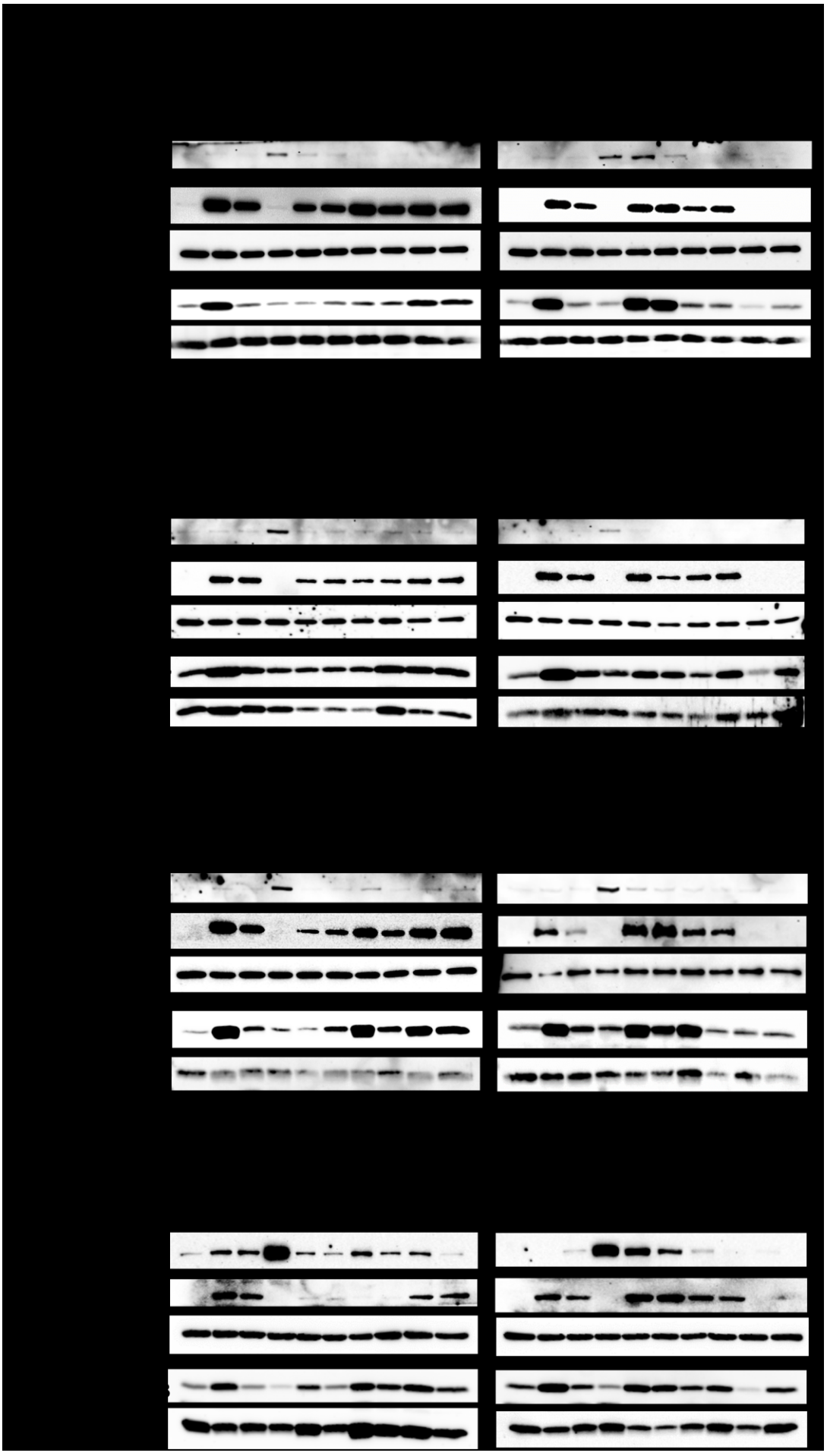

Figure 4. Western blot analysis in THP1, U937, K562, and MEK1 cell lines. **5c**, **5g**, **5h**, **5k**, **5j**, **5m** were used at 10 μM for 24h and 48h, and compared to CTR, **TUB**, **PCI** (tested at 10 μM) and **SAHA** (5 μM).

Therapeutic potential of new HDACis in acute human leukemia NB4 and MOLT-4 cells: proapoptotic effect

The HDAC6-sensitive NB4 and MOLT-4 leukemic cells were included in our screening panel (**Figure 5**) in order to evaluate the cell death mechanism (**Figure 6**) in comparison with the healthy human embryonic kidney HEK-293 cells (**Figure S1**). Increasing concentrations (1, 10, and 50 μM) of the compounds for 24, 48, and 72 h were assayed and **TUB**, **PCI**, and **SAHA** were used as reference HDACis at a concentration of 10 μM. In NB4 cells, a significant reduction in cell viability was observed for all the new compounds at 10 and 50 μM concentrations for the three incubation times, except for compound **5m** which was not able to significantly reduce cell viability after 24 h of incubation (**Figure 5A**). At a concentration of 1 μM, no effect was observed after 24 h of treatment with the new compounds, while a significant reduction was observed after 48 h of incubation for compounds **5c**, **5j**, **5g**, and **5k**, and at 72 h for compounds **5c**, **5g**, **5j**, **5k**, **5h**, and **5m**.

As evident from the IC_{50} values reported in the insert of **Figure 5A**, the most potent compounds were **5g** and **5h** after 72 h of incubation, molecules that preferentially bind HDAC6.

In NB4 cells, reference compounds at 10 μM promoted a reduction in cell viability at all incubation times except for **TUB** at 24 h. In human acute lymphoblastic leukemia cell line MOLT-4, no significant effect was observed at a concentration of 1 μM, except for **5k** (a dual HDAC6/HDAC1 inhibitor) at 72 h of incubation (**Figure 5B**). At concentrations of 10 and 50 μM, all tested inhibitors, with the exception of **5m**, significantly reduced cell viability at 24, 48, and 72 h. From the IC_{50} values reported in the insert of **Figure 5B**, the most potent compounds in MOLT-4 cells were **5c**, **5g** and **5k**, while, again, weak efficacy was

observed for **5m**.Among the reference compounds, only **SAHA** showed a significant effect in this cell line.

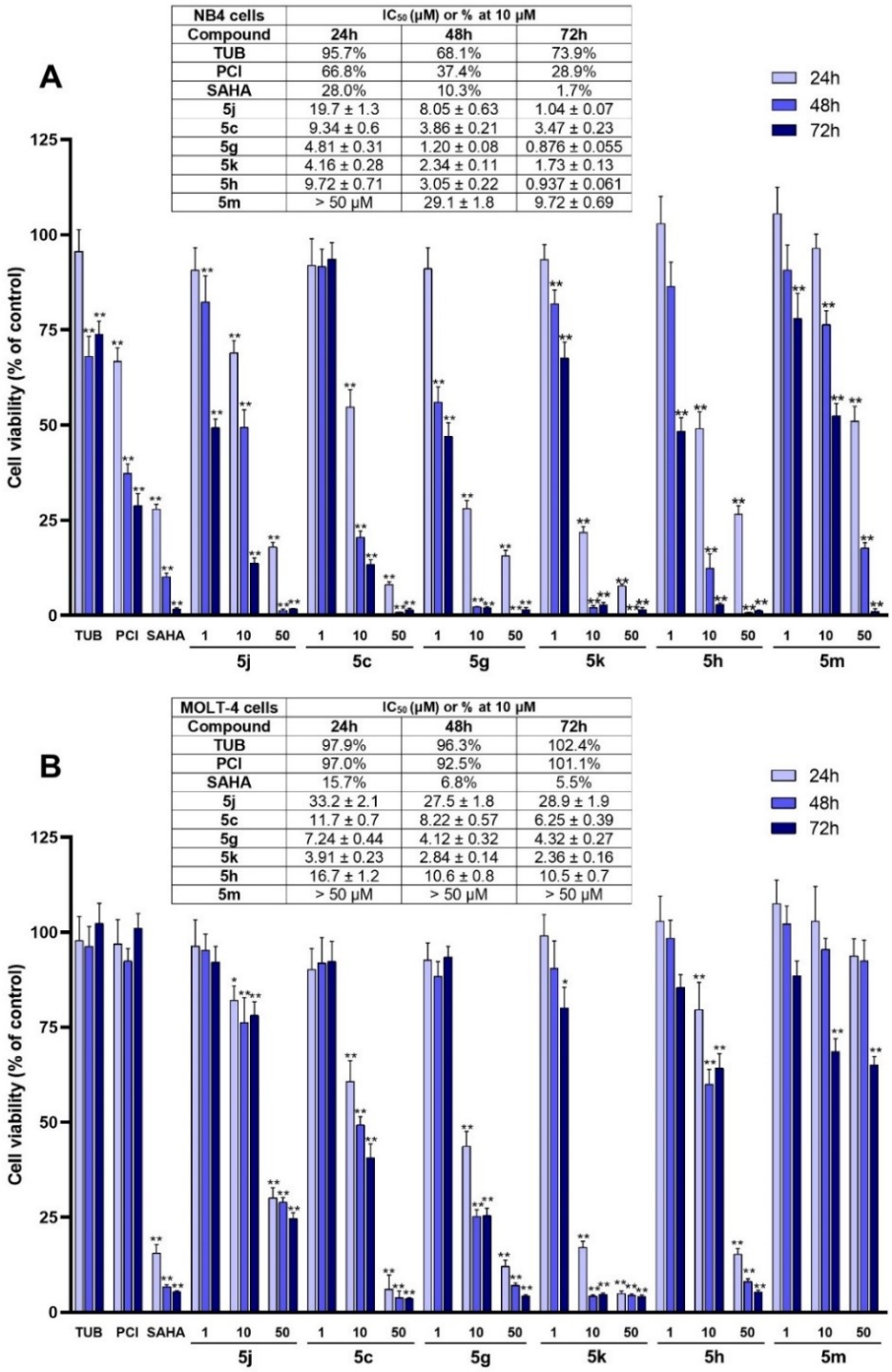

Figure 5. Effect of the novel HDACis on NB4 (A) and MOLT-4 (B) cell viability. MTT assays were performed by incubating the cells with 1, 10, and 50 μM concentrations of novel compounds and 10 μM of the reference compounds **TUB**, **PCI** and **SAHA** for 24, 48, and 72 h. Results are presented as a percentage of control for each incubation time and are expressed as the mean ± SEM of three independent experiments. The IC_{50} values of the novel HDACis and the percentage of cell viability for the reference compounds are reported in the inserts. *, $p<0.05$ and **, $p<0.01$ vs control.

These data highlight that **TUB** is not an interesting anticancer tool in leukemic tissues, pointing out the need for new selective HDACis with therapeutic potential in blood malignancies. In HEK-293 cells, used as reference healthy cells, a slight reduction of cell viability was observed with compounds **5c** and **5g** at 50 μM after 72 h of incubation. Among reference compounds, **SAHA** (10 μM) had significant effects on HEK-293 cell viability at 48 and 72 h after treatment (**Figure S1**). Induction of apoptosis after 24 h of treatment with the selected HDACis **5c**, **5g** and **5h** (representative of the family as preferential HDAC6is) was investigated in NB4 and MOLT-4 cells through the evaluation of caspase 3/7 activation (**Figure 6A-B**).

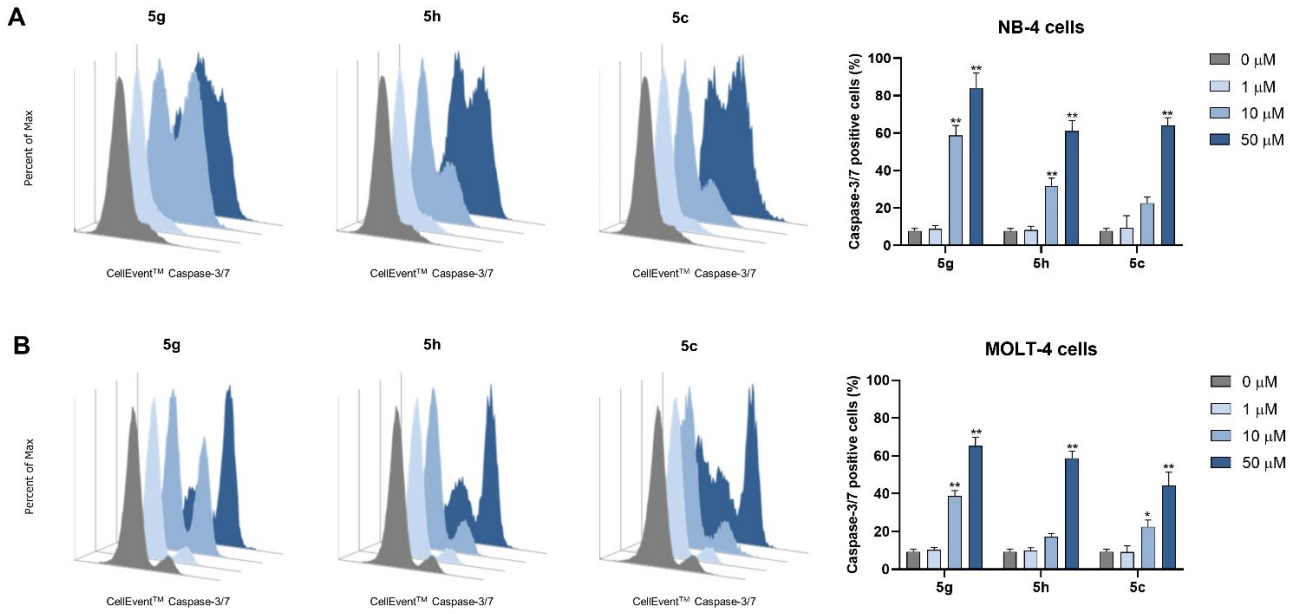

Figure 6. Activation of caspase 3/7 by selected compounds **5c**, **5g**, and **5h** in NB4 (A) and MOLT-4 (B). Cells were treated with the indicated concentrations of the novel compounds for 24 hours, labeled with CellEvent Caspase-3/7 Green Detection Reagent and analyzed by flow cytometry. The panels on the left report representative flow cytometric overlay histograms of caspase 3/7 activation while the panel on the right reports the percentage of caspase 3/7 positive cells expressed as the mean ± SEM of three independent experiments. *, $p<0.05$ and **, $p<0.01$ vs control (grey bar).

In NB4 cells, **5g** and **5h** significantly increased the percentage of caspase 3/7 positive cells both at 10 and 50 μM concentrations, while a significant effect was observed for compound **5c** at 50 μM concentration (**Figure 6A**). In MOLT-4 cells, **5c** and **5g** significantly

induced apoptosis at a concentration of 10 μM, while all the tested compounds significantly activated caspase 3/7 at 50 μM concentration (**Figure 6B**). These data, collected at 10 and 50 μM, indicate the possible engagement of different HDAC isoforms by the designed compounds.

Therapeutic potential of new HDACis in multiple myeloma and hairy cell leukemia cells: induction of apoptosis

In MM and B-cell lymphomas including HCL, HDAC6 is overexpressed through c-Myc signaling activation and upregulation of NF-κB, MAPK, and/or PI3K/AKT pathways, and its inhibition results in reduced tumor cell survival by promoting apoptosis and c-Myc downregulation.[48]

The compounds **5c**, **5g**, **5h**, **5j** and **5k** were tested in MM1.S (MM cell line), BONNA-12 (HCL cell line), and in primary healthy peripheral blood mononuclear cells (PBMCs) (**Figure 7B**), at various concentrations for 24, 48 and/or 72 h, and cell metabolic activity was assessed by MTT assay and IC_{50} calculated (**Figure 7A** and **Figure S2**), as well as viability and apoptosis, which were assessed by Annexin-V-PI through flow cytometry. After 48 h treatment, the IC_{50} values were calculated, in particular compound **5g** showed an IC_{50} value of 43.4 μM in MM.1S, 52.4 μM in BONNA-12, and 1.3 μM in healthy (3.01 μM at 72 h); similarly compound **5k** showed IC_{50} values of 14.6 μM in MM.1S, 41.8 μM in BONNA-12, and 6.5 μM in healthy (15.96 μM at 72 h); for **5c** IC_{50} was 18.4 μM in MM.1S, 14.3 μM in BONNA-12, and 1.2 μM in healthy (2.5 μM at 72 h); lower values were assessed for compounds **5h** with IC_{50} values of 1.3 μM in MM.1S, 10.3 μM in BONNA-12, and 6.3 μM in healthy (32.1 μM at 72 h); and for **5j** with IC_{50} values of 4.9 μM in MM.1S, 41.9 μM in BONNA-12, and 43.4 μM in healthy (2.5 μM at 72 h) (**Figure 7A**).

Apoptosis assay displayed different impacts of each HDAC inhibitor on cell lines (**Figure 7B**). Indeed, **5j** did not exert any effect on BONNA-12 cells at different incubation times

and tested concentrations (all $p > 0.05$), while the viability of healthy primary cells significantly decreased at higher concentrations (50 μM) and longer incubation time (72 h), as well as MM.1S cell viability which was significantly lowered only at high concentrations (50 μM) and after at least 48 h incubation (all $p < 0.05$). Conversely, **5c** displayed a significantly higher cytotoxicity already at 10 μM and after 24 h of treatment in MM.1S cell line (untreated vs 10 μM, $p = 0.0352$, $p = 0.0018$, and $p < 0.0001$, 24, 48 and 72 h of treatment), while cytotoxicity was observed only at higher concentrations (50 μM) in BONNA-12 cell line (untreated vs 50 μM, $p = 0.0466$ at both 24 h and 72 h of treatment) and in healthy PBMCs (untreated vs 50 μM, $p = 0.0221$ and $p = 0.0006$ at 48 h and 72 h of treatment).

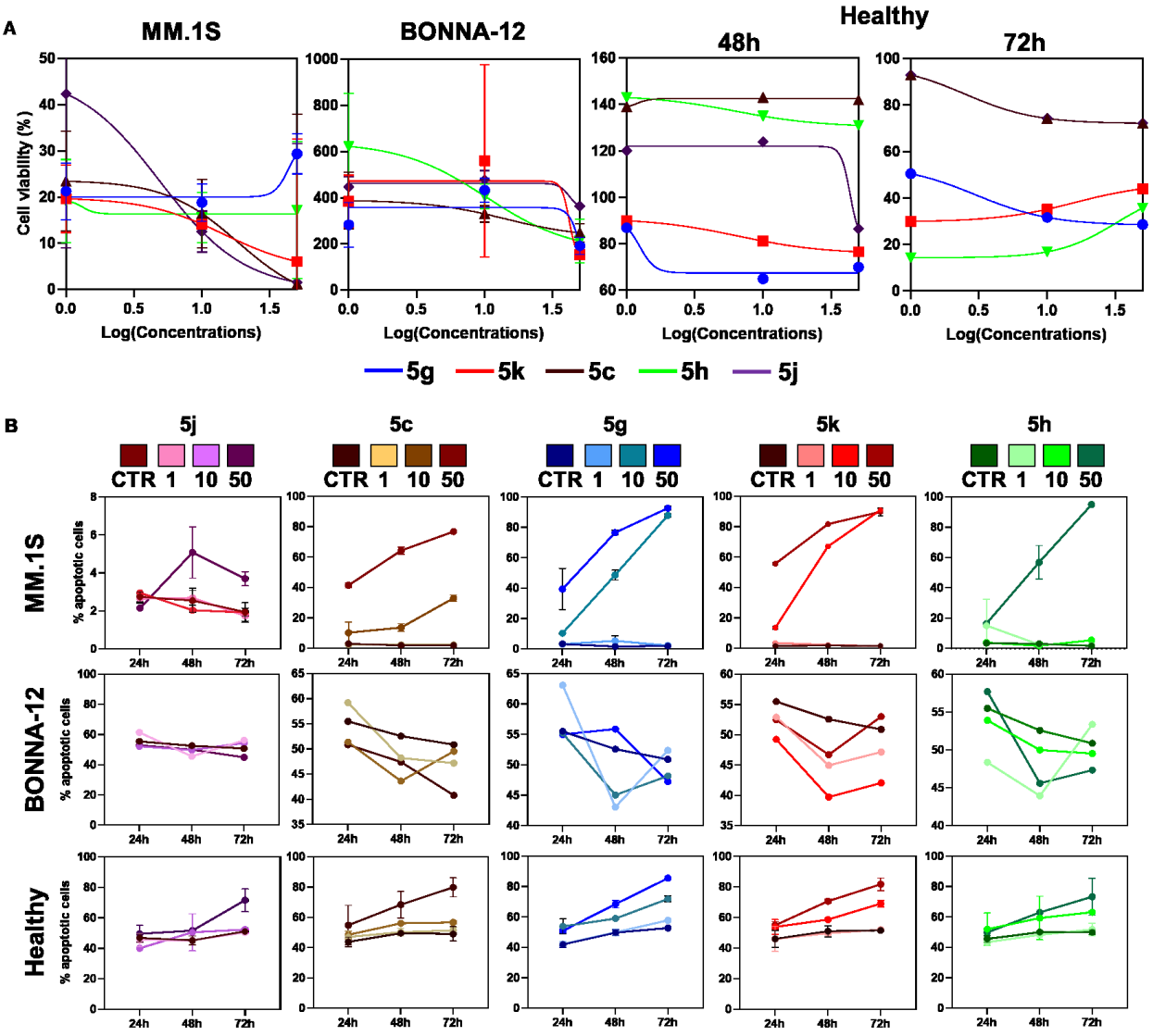

Figure 7. Viability assay in MM.1S, BONNA-12 cells and healthy PBMCs at 48 and/or 72 h of treatment for **5c, 5g, 5h, 5j** and **5k** compared to CTR.

Moreover, **5g** did not exert any cytotoxic effects on BONNA-12 cells (all $p < 0.05$), while it significantly influenced viability of MM.1S cells at 10 μM only after 48 h of treatment (untreated vs 10 μM, $p < 0.0001$ at 48h and 72 h of treatment) and of healthy PBMCs at 10 μM after at least 24 h of treatment (untreated vs 10 μM, $p = 0.0005$, $p = 0.0039$, and $p < 0.0001$, at 24 h, 48 h and 72 h of treatment).

An opposite behavior between MM and HCL cell line was observed for **5k**. Indeed, MM.1S exhibited a high susceptibility to **5k** starting from 10 μM and 24 h of treatment (all $p < 0.0001$), while cell viability was surprisingly increased in BONNA-12 starting from 1 μM of **5k** and 24 h of treatment (untreated vs 1 μM, $p = 0.0447$; and untreated vs 10 μM, $p = 0.0023$). Similarly to MM.1S cells, healthy PBMC viability was highly influenced by **5k** with increased apoptosis at 10 μM starting from 24 h of treatment (untreated vs 10 μM, $p = 0.0005$, $p = 0.0039$, and $p < 0.0001$, at 24 h, 48 h and 72 h of treatment). Among all HDAC inhibitors, **5h** was the less effective compound, with no cytotoxic effect on BONNA-12 cells (all $p > 0.05$), and with some cytotoxic effects only at higher concentrations (50 μM) at longer incubation times in MM.1S (at 48 h and 72 h of treatment, all $p < 0.0001$) and in healthy PBMCs (at 72 h, $p = 0.0160$) (**Figure 7B**).

According to these previous findings,[48] we confirmed the pro-apoptotic effects of HDAC6 inhibition in plasma cell disorders and B-cell neoplasms, especially in MM, likely because of a concomitant modulation of aggresomal pathway of protein degradation and unfolded-protein response, highly altered in MM cells.[49] Indeed, proteasome inhibitors are the hallmark in therapeutic treatment of MM patients, as neoplastic plasma cells produce large amounts of immunoglobulins that are degraded through misfolded/unfolded protein degradation mechanisms.[50]

HDAC6 binds to polyubiquitinated and coordinates the clearance of protein aggregates by modulating aggresome formation and their autophagic degradation through HSF1 and HSP90 activation.[51] Therefore, HDAC6 inhibition in MM could induce cell death by directly promoting apoptosis and by indirectly interfering with protein degradation mechanisms.

In more aggressive lymphomas, HDAC6 is highly expressed and mediates anti-apoptotic activities together with NF-κB signaling constitutive activation and Bcl-2 functions.[48] Conversely, in indolent B-cell neoplasia, such as follicular lymphoma, combination of HDAC6i A452 and ibrutinib leads to tumor cell apoptosis by downregulation of c-Myc and inactivation of Akt and ERK1/2 signaling.[52] In autoimmune disorders, such as systemic lupus erythematosus, autoantibody-producing plasma cells and germinal center autoreactive B cells are highly affected by HDAC6 inhibition, with a complete abrogation of abnormal B cell activation and differentiation and modulation of cellular metabolism pathways, such as fatty acid and glucose oxidation mechanisms.[53] From our results, HDAC6 inhibition seemed to exert more a cytostatic rather than a cytotoxic effect in HCL, likely because it might act more on B cell activation and differentiation, as occurring in systemic lupus, rather than pro-apoptotic trigger, as in aggressive lymphomas.

The new HDAC inhibitors rescue the hematopoietic phenotype of the FLT3-ITD zebrafish model of AML

After establishing that **5c**, **5g** and **5h** preferentially interfere with HDAC6 displaying proapoptotic potential in different blood malignancies, we progressed our investigation protocol studying their efficacy *in vivo* using a zebrafish AML model with FLT3-ITD mutation.[33] Prior to entering into *in vivo* experimentation, we confirmed the physicochemical properties of the new compounds in order to ascertain the possibility of administering these analogues to zebrafish in aqueous medium. The solubility and chemical stability of compounds **5c**, **5g** and **5h** compared with **5k** and **TUB** were

determined by HPLC methodology.[54,55] Solubility and chemical stability were measured at pH = 7.4 (**Table S1**) after 24 h. The compounds were stable at pH = 7.4; in particular, **5c** and **5h** displayed stability > 99%. In terms of solubility **5c** and **5h** performed better than **5g**, **5k** and **TUB**. The experimentally determined LogP values of **5c**, **5g** and **5h** highlighted that they could be used in the zf AML FLT3-ITD(+) model (**Table S1**).

We also evaluated the safety of the new inhibitors performing drug response assays in zebrafish embryos, which provide a suitable platform for high-throughput screening of new compounds. Since we were interested in defining the antileukemic profile of these compounds, we administrated the inhibitors from 1.5 days post fertilization (dpf), the developmental stages at which the leukemic phenotype is established in the AML zebrafish model, and evaluated the hematopoietic phenotype one day after the treatments.[23]

Tg(*CD41*:GFP) embryos expressing GFP in hematopoietic stem progenitor cells (HSPCs)[56] were exposed to different concentrations of **5c**, **5g** and **5h** and one day after the treatments, embryos were examined. We found that all HDACis were well tolerated up to a final concentration of 100 μM, since no significant differences were observed in terms of embryos survival (**Figure S3A**) and body axis formation in comparison to the DMSO-treated control embryos (**Figure S4A-E)**.

In addition, to further evaluate the effects of the compounds on embryo morphology and development, various parameters such as body length (**Figure S4F**), area of yolk (**Figure S4G)**, pericardium (**Figure S4H**) and eye (**Figure S4I**) districts were measured.

There were no significant differences in all the parameters investigated, when treated embryos were compared to the controls. In contrast, higher concentrations of tested compounds, negatively affect embryos survival (**Figure S3B**) and resulted in adverse effects, especially at the level of the pericardium (**Figure S3C-F**).

From these experiments, we defined 100 μM as the working dose for each compound to be used for the assessment of the antileukemic profile.

After establishing the working dose, we tested the compounds' efficacy in blocking the expansion of HSPCs, using the FLT3-ITD zebrafish model of AML (**Figure 8**). The FLT3-ITD *m*RNA and, as a control, the FLT3 wild-type (WT) *m*RNA were injected into 1 cell stage embryos of the Tg(*CD41*:GFP) line.

After the treatments, the expression of *cmyb*, another HSPCs marker,[57] was examined at the level of the caudal hematopoietic tissue (CHT), the site of definitive hematopoiesis at this stage of development (**Figure 8A**). The increased *cmyb* expression detected in the CHT of FLT3-ITD overexpressing embryos (**Figure 8B-C; G**), was reduced when the embryos were treated with the different HDACis (**Figure 8D-G)**.

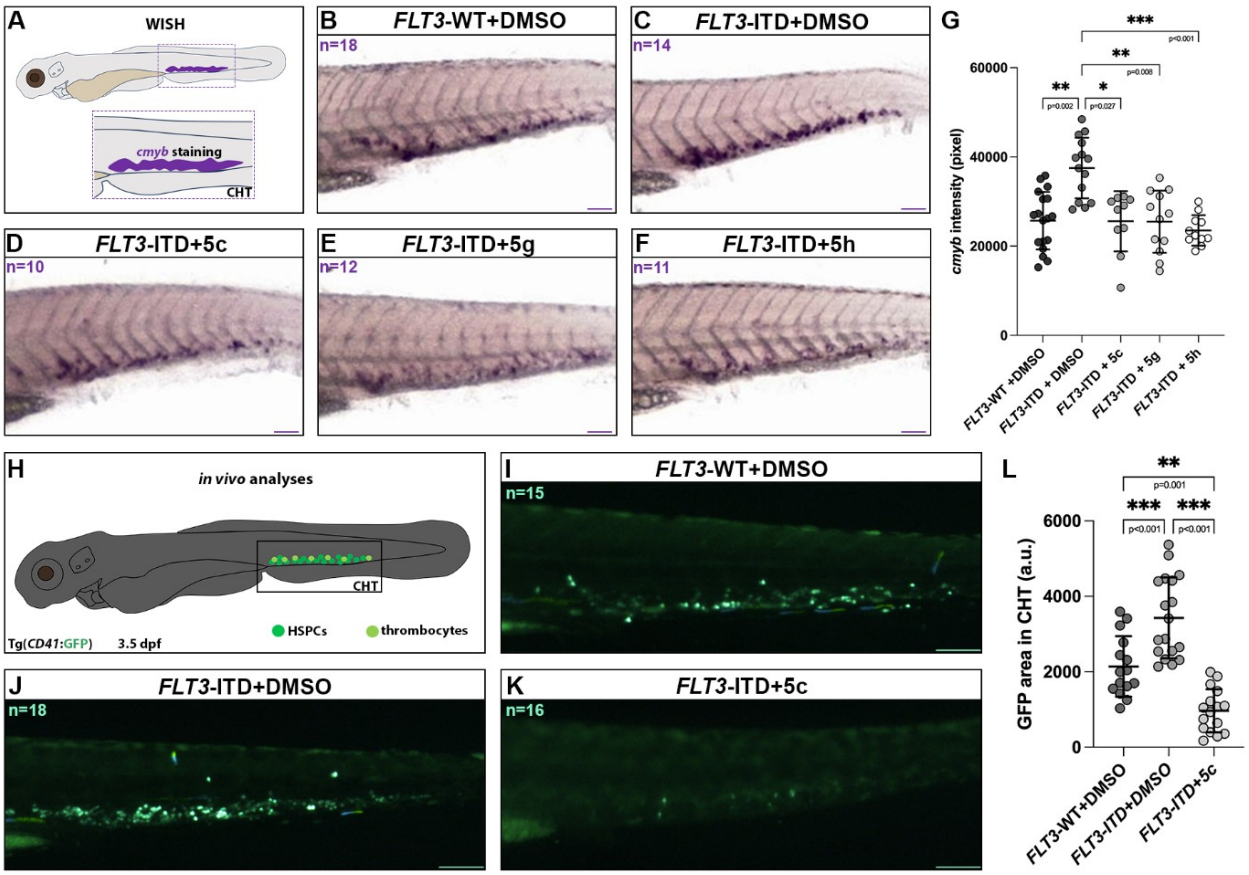

Figure 8. Effects of 5c, 5g and 5h on the HSPCs of *FLT3*-ITD zebrafish model of AML. **A**) Representation of the *cmyb* staining at the levels of the caudal hematopoietic tissue probe in embryos **B**) injected with FLT3-WT mRNA and treated with DMSO or **C-F**) with treated with **J**) DMSO or **K**) 100 µM **5c**. **L**) Quantification of the area occupied by the GFP signal at the level of the CHT. Scale bars indicate 100 mm. Data are presented as mean+/-standard deviation. Not-parametric ONE-Way ANOVA Kruskal Wallis multiple

comparison test with Dunn's correction. Confidence interval (CI) 95%. ns indicates not significant values with p-values higher than 0.05; ***p<0.001; **p<0.01 and *p<0.05. n indicates the number of embryos analyzed.

To further confirm that the reduced *cmyb* expression correlated to a decrease in the HSPCs expansion, we chose **5c** as a paradigmatic molecule.

The injection of the FLT3-ITD *m*RNA induced the expansion of the HSPCs in comparison to the control embryos injected with the FLT3 WT form (**Figure 8H-I; L**).

The administration of **5c** significantly rescued the HSPCs expansion of FLT3-ITD overexpressing embryos (**Figure 8J-K**).

The expression of *cmyb* was also used as a read-out to evaluate the potential of a new combination treatment based on HDAC6 inhibitors and the selective FLT3 inhibitors gilteritinib, currently used in clinic practice for treatment of *FLT3* mutated AML.[58] We treated the embryos with the HDAC6 inhibitor **5c** alone or in combination with gilteritinib from 2.5 to 3.5 dpf (**Figure 9A**), and **5c** administration enhanced the gilteritinib-induced reduction in *cmyb* expression (**Figure 9B-G**). These results demonstrate that the new HDAC6 inhibitors may provide a valuable alternative to be exploited for AML treatment. In addition, our experiments support the use of our AML zebrafish model as a platform for high throughput screening of new combination setting.[23,59]

New HDAC inhibitors show anticancer activity and therapeutic potential in AML-*FLT3* ITD patient samples

The results of *in vivo* zebrafish investigation highlighted that all the compounds were able to rescue the HSPCs expansion of FLT3-ITD overexpressing embryos. Thus, we selected **5c** (leuxinostat) as a representative of the series to test its efficacy in *ex vivo* experiments using FLT3-ITD AML cells derived from two patients.

We first evaluated the acetylation levels of histone and non-histone proteins after treatment with **5c** in normal and pathological conditions by WB analysis.

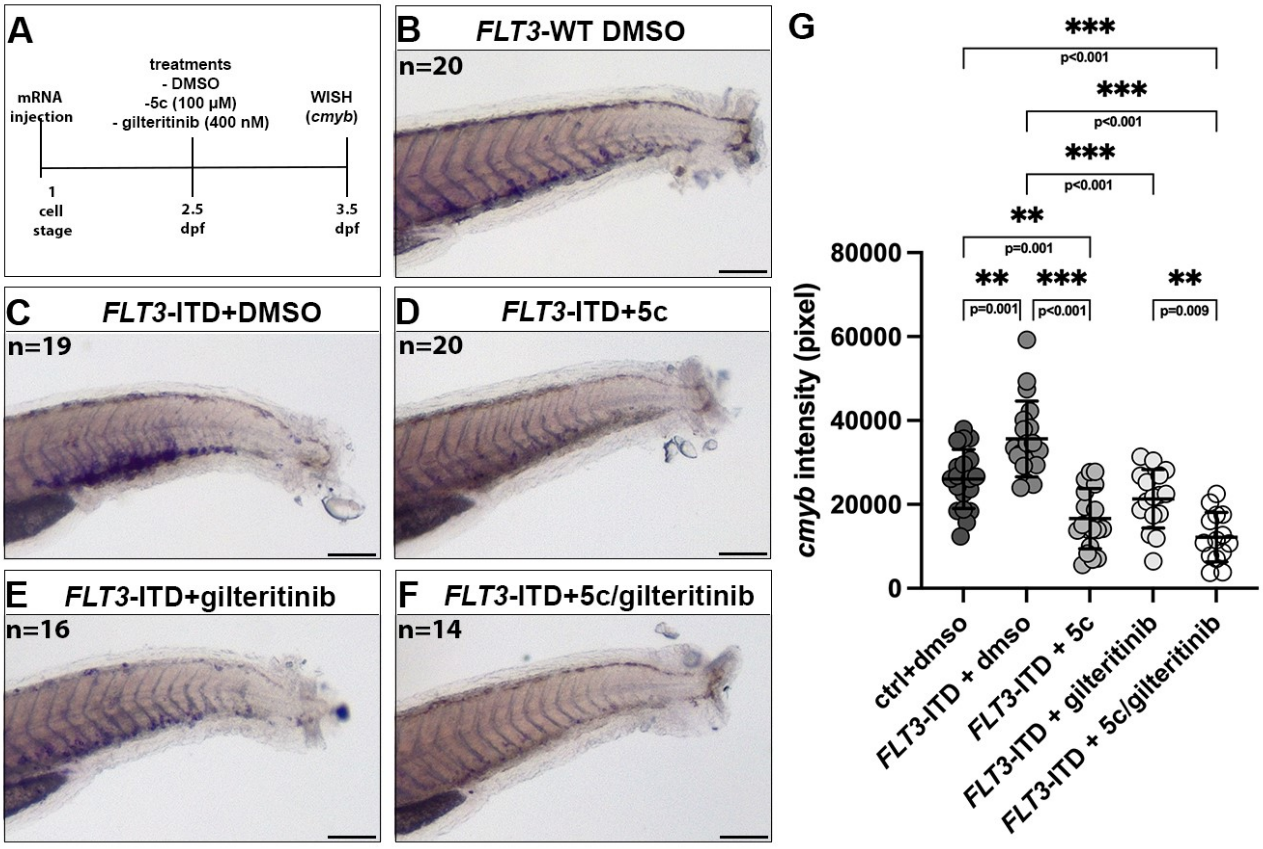

Figure 9. 5c in combination setting with the FLT3 selective inhibitor gilteritinib. A) Treatments timeline and doses used. **B-F**) Whole-mount *in situ* hybridization (WISH) with the *cmyb* probe in 3.5 dpf embryos. **B**) injected with *FLT3*-WT mRNA and treated with DMSO or **C-F**) with *FLT3*-ITD mRNA and treated with **C**) DMSO, **D**) 100 µM **5c**, **E**) 400 nM gilteritinib, **F**) 100 µM **5c** and 400 nM gilteritinib. **G**) Quantification of the *cmyb* staining in the different categories. Scale bars indicate 100 µm. Data are presented as mean+/- standard deviation. Normality of the distribution of the data was confirmed by Shapiro-Wilk test. ONE-Way ANOVA Tukey post hoc correction. Confidence interval (IC) 95%. not significant values with p-values higher than 0.05 were not shown; ***p<0.001; **p<0.01 and *p<0.05. n indicates the number of embryos analyzed.

Specifically, the acetylation levels of α-tubulin and histone H3K9/K14 were assessed after 48 h of treatment with **5c** or **SAHA** (clinically approved HDACi) at 10 µM (**Figure 10A**).

After treatment, **5c** significantly increased acetylation levels of α-tubulin in AML primary cells compared to untreated (p = 0.0128) and to positive controls (p = 0.0953) (**Figure**

10B,**C**), while no variations were observed in healthy PBMCs at tested concentrations (0, 1, 10, and 50 μM) and incubation time 48 and 72 h (all $p > 0.05$) (**Figure 10A** and **C**).

Conversely, no modifications were observed in AML cells for H3K9 acetylation, while only **SAHA** at 10 μM significantly induced the acetylation of H3K9/K14 in healthy PBMCs after 48h of treatment (10 μM **5c** vs 10 μM **SAHA**, $p = 0.0200$) (**Figure 10D**). These data underlined the differences between **5c** and **SAHA**, mainly based on the different HDAC inhibition profile.

Apoptosis was also tested by flow cytometry at 24 h and 48 h of treatment with **5c** at various concentrations (0, 1, 10, and 50 μM) or **SAHA** at 10 μM (**Figure 10E**). In healthy PBMCs, percentages of apoptotic, pre-apoptotic, and dead cells significantly augmented at increasing doses and incubation times (all $p < 0.0001$).

No variations were described in percentage of pre-apoptotic cells in AML at any concentration and time (all $p > 0.05$), while a slight increase in dead cells was observed at 24 h treatment with 10 μM of **5c** ($p = 0.0389$), with a corresponding decrease of apoptotic cells ($p = 0.0103$), confirmed also at 48 h of treatment (**Figure 10E**).

In AML, HDAC6 can be overexpressed together with Hedgehog proteins and multi-drug resistance genes. Specifically, HDAC6 mediates leukemic cell expansion, and its inhibition can restore physiological HSPC phenotype in both *NPM1* or FLT3-ITD AML models.[23]

Here, we reported a proof-of-concept of therapeutic potential of HDAC6 inhibition in FLT3 mutated AML B cells, as primary cells showed a typical HDAC6-mediated acetylation profile after **5c** treatment that could ultimately lead to apoptosis and reduction of leukemic cell expansion, as documented in primary cells and zebrafish model, respectively.

Effect of 5c on Langendorff perfused rat heart

Along the trajectory for the development of a novel optimized hit we usually perform tox studies (cell-based, functional assays and *in vivo*).

While low cytotoxic profile has been reported in **Figures S1-S2** (compounds **5c**,**5g**,**5h**,**5j**, **5k** and **5m**), and the scarce toxic potential has been determined *in vivo* in zebrafish (**Figure S3-S4** (compounds **5c**, **5g**, **5h**)), in this section we report experiments to evaluate cardiotoxicity.

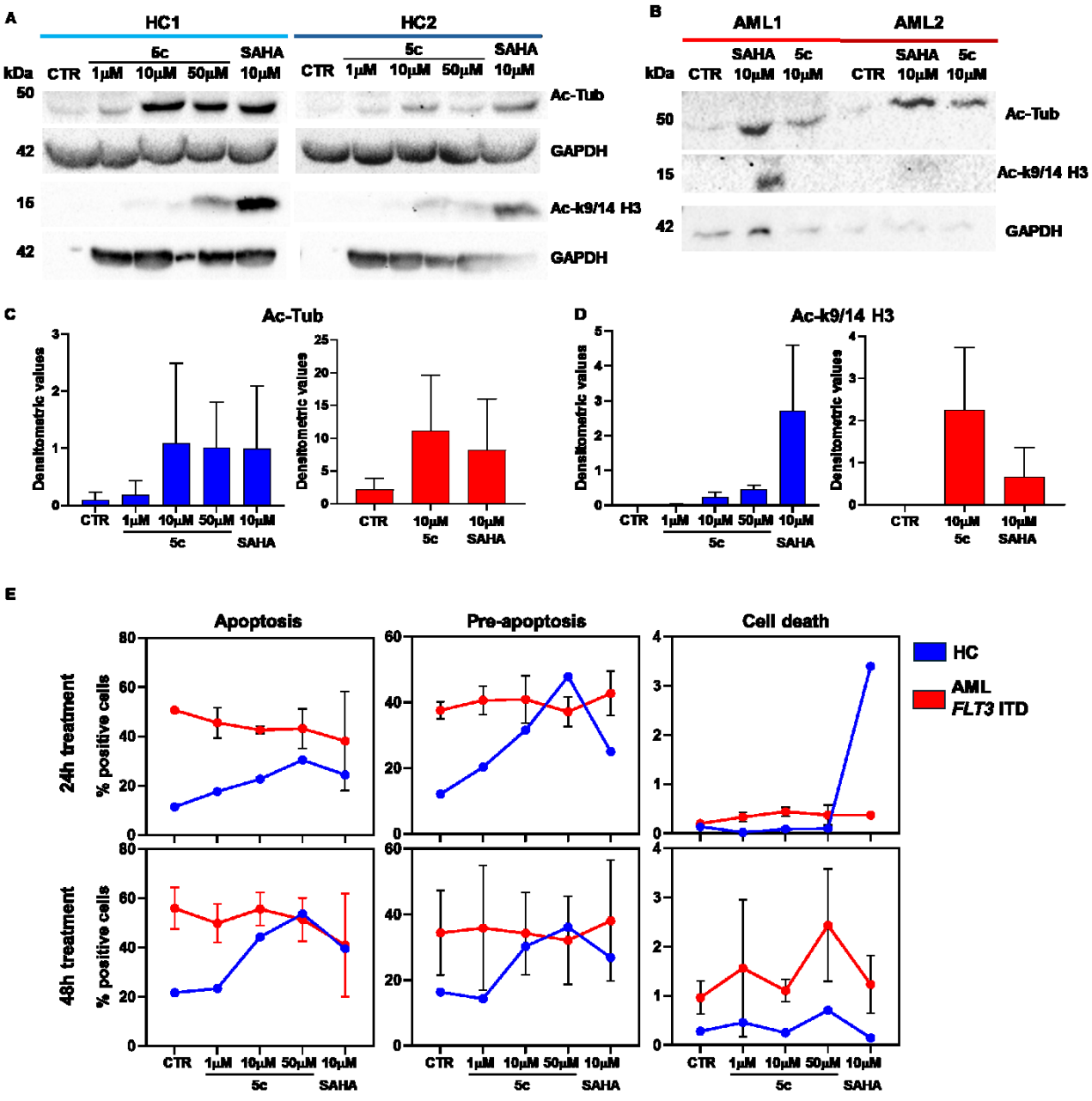

Figure 10. Efficacy of **5c** in AML FLT3-ITD cells from two AML patients. **A, B.** Immunoblot analysis of acetylated α-tubulin in postnuclear supernatants and acetylated histone H3-K9/14 in nuclear extracts of healthy cells (**A**) and leukemic cells (**B**) isolated from peripheral blood of FLT3-ITD AML patients. The stripped filters were reprobed with anti-GAPDH antibody. Molecular weights (kDa) are indicated on the left of the panels. **C,D**) Quantification of three independent experiments for acetylated α-tubulin (**C**) and acetylated histone H3-K9/14 (**D**). Mean±SD. **E**) Flow cytometric analysis of the percentage of

apoptosis in B cells purified from buffy coats of healthy donors (n ≥ 3) and FLT3-ITD AML patients One-way ANOVA test with multiple comparison. In each blot, the Precision Plus Protein™ Kaleidoscope™ Prestained Protein Standard was added for each subject.
The selected hit **5c** was evaluated in terms of cardiotoxic potential, by measuring its effect on cardiac mechanical function and electrocardiogram (ECG) in Langendorff-isolated rat hearts, as previously described.[60–62] Under control conditions, LVP and CPP values of 72.4 ± 9.2 and 53.6 ± 4.1 mmHg (n = 5), respectively, were obtained (**Figure S5**). Up to the highest concentration tested (50 μM), compound **5c** did not affect either LVP or CPP (**Figure S5**), nor the surface ECG (**Table S2**). The present findings highlight that **5c** was devoid of cardiac effects.

Conclusion

In this work, the development of new HDAC inhibitors (**5a-q**) has been reported. Some of them preferentially bind HDAC6, and their efficacy was tested in different blood cancer cell lines, including MM, CLL, HCL, and primary AML cells. These compounds interfered with cell viability of different leukemic cells, including THP-1, U937, K562, and MEK1 cells. In particular, our compounds promoted a marked acetylation of α-tubulin (a non-histone target of HDAC6) compared to histone H3 (an HDAC1-HDAC3 histone substrate) and SMC3 (a non-histone target of HDAC8). In HDAC6 sensitive NB4 and MOLT-4 cells, as well as in MM.1S and BONNA-12 cells, our molecules induced apoptosis as determined by caspases 3/7 cleavage experiments or by Annexin V/PI. *In vivo*, **5c**, **5g** and **5h** rescued normal hematopoietic phenotype in zebrafish FLT3-ITD AML model and the selected **5c** induced apoptosis in FLT3-ITD AML patients and a marked acetylation of α-tubulin compared to histone H3, indicating that at the tested doses, **5c** preferentially interfered with HDAC6 functions. Therefore, this new class of inhibitors could effectively induce FLT3 mutant cell apoptosis without affecting normal cell viability and without interfering with FLT3 kinase activities, consequently limiting potential side effects associated with direct

FLT3 inhibition. Furthermore, we provided additional evidence of a great clinical potential of HDAC inhibition in FLT3-ITD AML, and we investigated for the first time the efficacy of HDAC6 inhibitors in HCL. However, further *in vitro* and *in vivo* experiments are needed to translate our preliminary results into clinical practice.

Methods

Methods are reported in Supporting Information.[23,36,56,63–76]

Acknowledgements

Giuseppe Campiani, Stefania Butini and Giovanna Panzeca thank Next Generation EU – National Recovery and Resilience Plan (NRRP) – Mission 4 Component 2 Investment 1.4 – Italian Ministry of University and Research (MUR) Project Code ECS_00000017 MUR Directoral Decree n.1055 , 23 June 2022, CUP B83C22003930001, "Tuscany Health Ecosystem – THE" - Spokes 7-8. Giuseppe Campiani and Stefania Butini also thank Regione Toscana IT for the grant Bando Ricerca Salute 2018-Regione Toscana - PRECISE-CLL, "Development of personalized diagnosis and innovative therapies for resistant CLL". Rosaria Benedetti, Lucia Altucci and Ugo Chianese thank NRRP-MAD-2022-12376723; NRRP-CN3, National Centre for Gene Therapy and Drugs-Based on RNA Technology, cod: CN000000041. Anna Pistocchi, Alex Pezzotta and Giuseppe Campiani thank AIRC-Investigator Grant- IG 2023, code 29187.
We acknowledge Jona Ximerti (University of Milan) for her priceless support in performing preliminary analysis in zebrafish.

Author Information

Gabriele Carullo 0000-0002-1619-3295 gabriele.carullo@unisi.it
Sara Rossi 0000-0002-8240-6519 rossi115@student.unisi.it
Valentina Giudice 0000-0002-7492-6848 vgiudice@unisa.it
Alex Pezzotta 0000-0003-1788-5880 alex.pezzotta@unimi.it
Ugo Chianese 0000-0003-2726-1895 ugo.chianese@unicampania.it
Pasqualina Scala 0000-0001-6292-4186 pscala@unisa.it
Anna Fontana 0000-0002-5091-8202 a.fontana5@student.unisi.it
Giovanna Panzeca 0000-0001-6479-7686 giovanna.panzeca@unisi.it
Silvia Pasquini 0000-0001-9442-1428 psqslv@unife.it
Chiara Contri 0000-0003-3936-5923 chiara.contri@unife.it
Sandra Gemma 0000-0002-8313-2417 gemma@unisi.it
Anna Ramunno 0000-0003-1089-2439 aramunno@unisa.it
Simona Saponara 0000-0002-3831-8669 simona.saponara@unisi.it
Francesca Galvani 0000-0002-7543-9945 francesca.galvani@unipr.it
Alessio Lodola 0000-0002-8675-1002 alessio.lodola@unipr.it
Marco Mor 0000-0003-0199-1849 marco.mor@unipr.it
Rosaria Benedetti 0000-0001-5517-5519 rosaria.benedetti@unicampania.it
Carmine Selleri 0000-0002-5861-8984 cselleri@unisa.it
Katia Varani 0000-0003-4562-1348 vrk@unife.it

Stefania Butini 0000-0002-8471-0880 butini3@unisi.it
Lucia Altucci 0000-0002-7312-5387 lucia.altucci@unicampania.it
Fabrizio Vincenzi 0000-0002-5027-1699 fabrizio.vincenzi@unife.it
Anna Pistocchi 0000-0001-9467-2542 anna.pistocchi@unimi.it
Giuseppe Campiani 0000-0001-5295-9529 campiani@unisi.it

*Corresponding authors
Prof. Sandra Gemma, Department of Biotechnology, Chemistry and Pharmacy, University of Siena, E-mail: gemma@unisi.it
Prof. Giuseppe Campiani, Department of Biotechnology, Chemistry and Pharmacy, University of Siena E-mail: campiani@unisi.it
# Gabriele Carullo and Sara Rossi contributed equally

References

(1) An, Z.-Y.; Fu, H.; He, Y.; Zhu, X.; Huang, Q.-S.; Wu, J.; Liu, K.; Zhang, X. Projected Global Trends in Hematological Malignancies: Incidence, Mortality, and Disability-Adjusted Life Years from 2020 to 2030. *Blood* **2023**, *142* (Supplement 1), 3810–3810. https://doi.org/10.1182/BLOOD-2023-187856.

(2) Zhang, N.; Wu, J.; Wang, Q.; Liang, Y.; Li, X.; Chen, G.; Ma, L.; Liu, X.; Zhou, F. Global Burden of Hematologic Malignancies and Evolution Patterns over the Past 30 Years. *Blood Cancer Journal 2023 13:1* **2023**, *13* (1), 1–13. https://doi.org/10.1038/s41408-023-00853-3.

(3) Höpken, U. E.; Rehm, A. Targeting the Tumor Microenvironment of Leukemia and Lymphoma. *Trends Cancer* **2019**, *5* (6), 351–364. https://doi.org/10.1016/J.TRECAN.2019.05.001.

(4) Baeker Bispo, J. A.; Pinheiro, P. S.; Kobetz, E. K. Epidemiology and Etiology of Leukemia and Lymphoma. *Cold Spring Harb Perspect Med* **2020**, *10* (6). https://doi.org/10.1101/cshperspect.a034819.

(5) Fowlkes, S.; Murray, C.; Fulford, A.; Gelder, T. De; Siddiq, N. Myeloproliferative Neoplasms (MPNs) – Part 2: A Nursing Guide to Managing the Symptom Burden of MPNs. *Canadian Oncology Nursing Journal / Revue canadienne de soins infirmiers en oncologie* **2018**, *28* (4), 276–281. https://doi.org/10.5737/23688076284276281.

(6) Rossi, S.; Tatangelo, V.; Dichiara, M.; Butini, S.; Gemma, S.; Brogi, S.; Pasquini, S.; Cappello, M.; Vincenzi, F.; Varani, K.; Lopresti, L.; Malchiodi, M.; Carrara, C.; Gozzetti, A.; Bocchia, M.; Marotta, G.; Patrussi, L.; Carullo, G.; Baldari, C. T.; Campiani, G. A Novel Potent Class I HDAC Inhibitor Reverses the STAT4/P66Shc Apoptotic Defect in B Cells from Chronic Lymphocytic Leukemia Patients. *Biomedicine & Pharmacotherapy* **2024**, *174*, 116537. https://doi.org/10.1016/J.BIOPHA.2024.116537.

(7) Hammond, W. A.; Swaika, A.; Menke, D.; Tun, H. W. Hairy Cell Lymphoma: A Potentially under-Recognized Entity. *Rare Tumors* **2017**, *9* (1), 1–3. https://doi.org/10.4081/RT.2017.6518/ASSET/IMAGES/LARGE/10.4081_RT.2017.6518-FIG1.JPEG.

(8) Maitre, E.; Bertrand, P.; Maingonnat, C.; Viailly, P.-J.; Wiber, M.; Naguib, D.; Salaün, V.; Cornet, E.; Damaj, G.; Sola, B.; Jardin, F.; Troussard, X.; Maitre, E.; Bertrand, P.; Maingonnat, C.; Viailly, P.-J.; Wiber, M.; Naguib, D.; Salaün, V.; Cornet, E.; Damaj, G.; Sola, B.; Jardin, F.; Troussard, X. New Generation Sequencing of Targeted Genes in the Classical and the Variant Form of Hairy Cell Leukemia Highlights Mutations in Epigenetic Regulation Genes. *Oncotarget* **2018**, *9* (48), 28866–28876. https://doi.org/10.18632/ONCOTARGET.25601.

(9) Tiacci, E.; De Carolis, L.; Simonetti, E.; Capponi, M.; Ambrosetti, A.; Lucia, E.; Antolino, A.; Pulsoni, A.; Ferrari, S.; Zinzani, P. L.; Ascani, S.; Perriello, V. M.; Rigacci, L.; Gaidano, G.; Della Seta, R.; Frattarelli, N.; Falcucci, P.; Foà, R.; Visani, G.; Zaja, F.; Falini, B. Vemurafenib plus Rituximab in Refractory or Relapsed Hairy-Cell Leukemia. *New England Journal of Medicine* **2021**, *384* (19), 1810–1823. https://doi.org/10.1056/NEJMOA2031298/SUPPL_FILE/NEJMOA2031298_DATA-SHARING.PDF.

(10) Moreno Rueda, L. Y.; Bryant, D.; Tapper, W. J.; Weston-Bell, N. J.; Wedge, D. C.; Ansari-Pour, N.; Sahota, S. S. The Genomic Landscape and Clonal Evolutionary Trajectory of Classical Hairy Cell Leukemia. *Leukemia 2023 37:4* **2023**, *37* (4), 929–933. https://doi.org/10.1038/s41375-023-01823-1.

(11) Gargiulo, E.; Giordano, M.; Niemann, C. U.; Moussay, E.; Paggetti, J.; Morande, P. E. The Protective Role of the Microenvironment in Hairy Cell Leukemia Treatment: Facts and Perspectives. *Front Oncol* **2023**, *13*. https://doi.org/10.3389/FONC.2023.1122699.

(12) Diaz, R.; Vazquez Martinez, J. L. ; Khimani, M. ; New, F.; Roman Diaz, J. L.; Vazquez Martinez, M.; Khimani, F. New Approaches for the Treatment of AML beyond the 7+3 Regimen: Current Concepts and New Approaches. *Cancers 2024, Vol. 16, Page 677* **2024**, *16* (3), 677. https://doi.org/10.3390/CANCERS16030677.

(13) Dozzo, A.; Galvin, A.; Shin, J. W.; Scalia, S.; O'Driscoll, C. M.; Ryan, K. B. Modelling Acute Myeloid Leukemia (AML): What's New? A Transition from the Classical to the Modern. *Drug Delivery and Translational Research 2022 13:8* **2022**, *13* (8), 2110–2141. https://doi.org/10.1007/S13346-022-01189-4.

(14) Kayser, S.; Levis, M. J. The Clinical Impact of the Molecular Landscape of Acute Myeloid Leukemia. *Haematologica* **2023**, *108* (2), 308–320. https://doi.org/10.3324/HAEMATOL.2022.280801.

(15) Döhner, H.; Estey, E.; Grimwade, D.; Amadori, S.; Appelbaum, F. R.; Büchner, T.; Dombret, H.; Ebert, B. L.; Fenaux, P.; Larson, R. A.; Levine, R. L.; Lo-Coco, F.; Naoe, T.; Niederwieser, D.; Ossenkoppele, G. J.; Sanz, M.; Sierra, J.; Tallman, M. S.; Tien, H. F.; Wei, A. H.; Löwenberg, B.; Bloomfield, C. D. Diagnosis and Management of AML in Adults: 2017 ELN Recommendations from an International Expert Panel. *Blood* **2017**, *129* (4), 424–447. https://doi.org/10.1182/BLOOD-2016-08-733196.

(16) Song, M. K.; Park, B. B.; Uhm, J. E. Clinical Efficacies of FLT3 Inhibitors in Patients with Acute Myeloid Leukemia. *Int J Mol Sci* **2022**, *23* (20). https://doi.org/10.3390/IJMS232012708.

(17) Levis, M. J.; Perl, A. E.; Schiller, G. J.; Fathi, A. T.; Roboz, G. J.; Wang, E. S.; Altman, J. K.; Rajkhowa, T.; Ando, M.; Suzuki, T.; Subach, R. A.; Maier, G.; Madden, T.; Johansen, M.; Cheung, K.; Kurman, M.; Smith, C. C. A Phase 1 Study of the Irreversible FLT3 Inhibitor FF-10101 in Relapsed or Refractory Acute Myeloid Leukemia. *Blood Adv* **2024**. https://doi.org/10.1182/BLOODADVANCES.2023010619.

(18) Levis, M. J.; Hamadani, M.; Logan, B.; Jones, R. J.; Singh, A. K.; Litzow, M.; Wingard, J. R.; Papadopoulos, E. B.; Perl, A. E.; Soiffer, R. J.; Ustun, C.; Ueda Oshima, M.; Uy, G. L.; Waller, E. K.; Vasu, S.; Solh, M.; Mishra, A.; Muffly, L.; Kim, H.-J.; Mikesch, J.-H.; Najima, Y.; Onozawa, M.; Thomson, K.; Nagler, A.; Wei, A. H.; Marcucci, G.; Geller, N. L.; Hasabou, N.; Delgado, D.; Rosales, M.; Hill, J.; Gill, S. C.; Nuthethi, R.; King, D.; Wittsack, H.; Mendizabal, A.; Devine, S. M.; Horowitz, M. M.; Chen, Y.-B.; Agura, E.; Altman, J.; Anagnostopoulos, A.; Anand, S.; Artz, A.; Aulitzky, W.; Balderman, S.; Ballen, K.; Becker, M.; Beguin, Y.; Berkahn, L.; Berneman, Z.; Bhatt, V.; Bilmon, I.; Bonifazi, F.; Briggs, A.; Bruno, B.; Brunstein, C.; Byrne, M.; Byrne, J.; Cabrero, M.; Cairoli, R.; Carrum, G.; Cerny, J.; Chen, Y.-B.; Cheong, J.-W.; Ciceri, F.; Colorado, M.; Cook, R.; Couriel, D.; Craddock, C.; Damon, L.; Deol, A.; Desbrosses, Y.; Devine, S.; Di Grazia, C.; Di Stasi, A.; Dias, A.; Dorritie, K.; Essell, J.; Eto, T.; Farag, S.; Forcade, E.; Frankfurt, O.; Fujiwara, S.; Fukuda, T.; Fukushima, K.; Furst, S.; Goto, T.; Hall, A.; Hatta, S.; Hicheri, Y.; Horwitz, M.; Hou, H.-A.; How, J.; Howard, D.; Hsu, W.-H. (Blake); Huynh, A.; Irvine, D.;

Ishikawa, T.; Jamieson, K.; Jedrzejczak, W.; Jethava, Y.; Jimenez, A.; Jung, C. W.; Kanda, J.; Karakasis, D.; Kato, J.; Kekre, N.; Khera, N.; Kim, H.-J.; Klein, A.; Kobbe, G.; Kornblit, B.; Kota, V.; Lachance, S.; Leber, B.; Lee, C.; Lee, J. H.; Levis, M. J.; Lin, T.-L.; Litzow, M.; Liu, T.-C.; Martelli, M.; Martinez, C.; Matsuoka, K.; McCarty, J.; Mendez, L.; Michelis, F.; Mikesch, J.-H.; Mineishi, S.; Mishra, A.; Mohty, M.; Moors, I.; Motyckova, G.; Mueller, L.; Muffly, L.; Najima, Y.; Nakamae, H.; Nakano, N.; Nathan, S.; Nicholson, E.; Norkin, M.; Ogawa, Y.; Olesen, G.; Oluwole, O.; Onozawa, M.; Pantin, J.; Papadopoulos, E. B.; Paulson, K.; Pemberton, L.; Perera, T.; Perl, A. E.; Piatkowska-Jakubas, B.; Poire, X.; Protheroe, R.; Rambaldi, A.; Ritchie, D.; Ross, K.; Rubio, M.-T.; Santarone, S.; Sanz Caballer, J.; Sawa, M.; Schaar, D.; Scheid, C.; Schriber, J.; Seropian, S.; Shah, N.; Shah, N.; Shore, T.; Gil, J. S.; Singh, A.; Sobecks, R.; Socie, G.; Soiffer, R.; Solh, M.; Sprague, K.; Spyridonidis, A.; Stelljes, M.; Stiff, P.; Stuart, R.; Tanaka, M.; Tandra, A.; Tholouli, E.; Thomas, X.; Thomson, K.; Tiribelli, M.; Tomlinson, B.; Tsirigotis, P.; Tzachanis, D.; Uchida, N.; Ueda, M.; Ustun, C.; Uy, G. L.; Valcarcel Ferreiras, D.; Vasu, S.; Wagner, E.; Waller, E. K.; Watson, A.-M.; Weisdorf, D.; Wingard, J. R.; Wolschke, C.; Wrobel, T.; Yakoub-Agha, I.; Yamauchi, T.; Yared, J.; Yeh, S.-P.; Yoon, S.-S.; Yoshihara, S. Gilteritinib as Post-Transplant Maintenance for Acute Myeloid Leukemia With Internal Tandem Duplication Mutation of FLT3. *https://doi.org/10.1200/JCO.23.02474* **2024**. https://doi.org/10.1200/JCO.23.02474.

(19) Wang, Z.; Cai, J.; Cheng, J.; Yang, W.; Zhu, Y.; Li, H.; Lu, T.; Chen, Y.; Lu, S. FLT3 Inhibitors in Acute Myeloid Leukemia: Challenges and Recent Developments in Overcoming Resistance. *J Med Chem* **2021**, *64* (6), 2878–2900. https://doi.org/10.1021/ACS.JMEDCHEM.0C01851/ASSET/IMAGES/MEDIUM/JM0C01851_0019.GIF.

(20) Zhao, J. C.; Agarwal, S.; Ahmad, H.; Amin, K.; Bewersdorf, J. P.; Zeidan, A. M. A Review of FLT3 Inhibitors in Acute Myeloid Leukemia. *Blood Rev* **2022**, *52*, 100905. https://doi.org/10.1016/J.BLRE.2021.100905.

(21) Desikan, S. P.; Daver, N.; DiNardo, C.; Kadia, T.; Konopleva, M.; Ravandi, F. Resistance to Targeted Therapies: Delving into FLT3 and IDH. *Blood Cancer Journal 2022 12:6* **2022**, *12* (6), 1–8. https://doi.org/10.1038/s41408-022-00687-5.

(22) Yang, H.; Maddipoti, S.; Quesada, A.; Bohannan, Z.; Cabrero Calvo, M.; Colla, S.; Wei, Y.; Estecio, M.; Wierda, W.; Bueso-Ramos, C.; Garcia-Manero, G. Analysis of Class I and II Histone Deacetylase Gene Expression in Human Leukemia. *Leuk Lymphoma* **2015**, *56* (12), 3426–3433. https://doi.org/10.3109/10428194.2015.1034705.

(23) Pezzotta, A.; Gentile, I.; Genovese, D.; Totaro, M. G.; Battaglia, C.; Leung, A. Y. H.; Fumagalli, M.; Parma, M.; Cazzaniga, G.; Fazio, G.; Alcalay, M.; Marozzi, A.; Pistocchi, A. HDAC6 Inhibition Decreases Leukemic Stem Cell Expansion Driven by Hedgehog Hyperactivation by Restoring Primary Ciliogenesis. *Pharmacol Res* **2022**, *183*, 106378. https://doi.org/10.1016/J.PHRS.2022.106378.

(24) Pietschmann, K.; Bolck, H. A.; Buchwald, M.; Spielberg, S.; Polzer, H.; Spiekermann, K.; Bug, G.; Heinzel, T.; Bo̎hmer, F. D.; Krämer, O. H. Breakdown of the FLT3-ITD/STAT5 Axis and Synergistic Apoptosis Induction by the Histone Deacetylase Inhibitor Panobinostat and FLT3-Specific Inhibitors. *Mol Cancer Ther* **2012**, *11* (11), 2373–2383. https://doi.org/10.1158/1535-7163.MCT-12-0129.

(25) Fontana, A.; Cursaro, I.; Carullo, G.; Gemma, S.; Butini, S.; Campiani, G. A Therapeutic Perspective of HDAC8 in Different Diseases: An Overview of Selective Inhibitors. *International Journal of Molecular Sciences 2022, Vol. 23, Page 10014* **2022**, *23* (17), 10014. https://doi.org/10.3390/IJMS231710014.

(26) Carullo, G.; Federico, S.; Relitti, N.; Gemma, S.; Butini, S.; Campiani, G. Retinitis Pigmentosa and Retinal Degenerations: Deciphering Pathways and Targets for Drug Discovery and Development. *ACS Chem Neurosci 11* (15), 2173–2191. https://doi.org/10.1021/acschemneuro.0c00358.

(27) Wachholz, V.; Mustafa, A. H. M.; Zeyn, Y.; Henninger, S. J.; Beyer, M.; Dzulko, M.; Piée-Staffa, A.; Brachetti, C.; Haehnel, P. S.; Sellmer, A.; Mahboobi, S.; Kindler, T.; Brenner, W.; Nikolova, T.; Krämer, O. H. Inhibitors of Class I HDACs and of FLT3 Combine Synergistically against Leukemia Cells with Mutant FLT3. *Arch Toxicol* **2022**, *96* (1), 177–193. https://doi.org/10.1007/S00204-021-03174-1/FIGURES/5.

(28) Pietschmann, K.; Bolck, H. A.; Buchwald, M.; Spielberg, S.; Polzer, H.; Spiekermann, K.; Bug, G.; Heinzel, T.; Bo̎mer, F. D.; Krämer, O. H. Breakdown of the FLT3-ITD/STAT5 Axis and Synergistic Apoptosis Induction by the Histone Deacetylase Inhibitor Panobinostat and FLT3-Specific Inhibitors. *Mol Cancer Ther* **2012**, *11* (11), 2373–2383. https://doi.org/10.1158/1535-7163.MCT-12-0129/84574/AM/BREAKDOWN-OF-THE-FLT3-ITD-STAT5-AXIS-AND.

(29) Bystrom, R.; Levis, M. J. An Update on FLT3 in Acute Myeloid Leukemia: Pathophysiology and Therapeutic Landscape. *Curr Oncol Rep* **2023**, *25* (4), 369–378. https://doi.org/10.1007/S11912-023-01389-2/METRICS.

(30) Ghai, V.; Sharma, K.; Abbi, K. K. S.; Shimko, S.; Epner, E. M. Combination Therapy with Cladribine, Vorinostat, and Ofatumumab Achieves Complete Hematologic Remission in Refractory Classical Hairy Cell Leukemia. *Blood* **2011**, *118* (21), 4622. https://doi.org/10.1182/BLOOD.V118.21.4622.4622.

(31) Deng, Y.; Cheng, Q.; He, J. HDAC Inhibitors: Promising Agents for Leukemia Treatment. *Biochem Biophys Res Commun* **2023**, *680*, 61–72. https://doi.org/10.1016/J.BBRC.2023.09.023.

(32) Ho, T. C. S.; Chan, A. H. Y.; Ganesan, A. Thirty Years of HDAC Inhibitors: 2020 Insight and Hindsight. *J Med Chem* **2020**, *63* (21), 12460–12484. https://doi.org/10.1021/acs.jmedchem.0c00830.

(33) He, B. L.; Shi, X.; Man, C. H.; Ma, A. C. H.; Ekker, S. C.; Chow, H. C. H.; So, C. W. E.; Choi, W. W. L.; Zhang, W.; Zhang, Y.; Leung, A. Y. H. Functions of Flt3 in Zebrafish Hematopoiesis and Its Relevance to Human Acute Myeloid Leukemia. *Blood* **2014**, *123* (16), 2518–2529. https://doi.org/10.1182/BLOOD-2013-02-486688.

(34) Campiani, G.; Cavella, C.; Osko, J.; Brindisi, M.; Relitti, N.; Brogi, S.; Saraswati, A. P.; Federico, S.; Chemi, G.; Maramai, S.; Carullo, G.; Jaeger, B.; Carleo, A.; Benedetti, R.; Sarno, F.; Lamponi, S.; Rottoli, P.; Bargagli, E.; Bertucci, C.; Tedesco, D.; Herp, D.; Senger, J.; Ruberti, G.; Saccoccia, F.; Saponara, S.; Gorelli, B.; Valoti, M.; Kennedy, B.; Sundaramurthi, H.; Butini, S.; Jung, M.; Roach, K.; Altucci, L.; Bradding, P.; Christianson, D.; Gemma, S.; Prasse, A. Harnessing the Role of HDAC6 in Idiopathic Pulmonary Fibrosis: Design, Synthesis, Structural Analysis, and Biological Evaluation of Potent Inhibitors. *J Med Chem 64* (14), 9960–9988. https://doi.org/10.1021/acs.jmedchem.1c00184.

(35) Papa, A.; Cursaro, I.; Pozzetti, L.; Contri, C.; Cappello, M.; Pasquini, S.; Carullo, G.; Ramunno, A.; Gemma, S.; Varani, K.; Butini, S.; Campiani, G.; Vincenzi, F. Pioneering First-in-Class FAAH-HDAC Inhibitors as Potential Multitarget Neuroprotective Agents. *Arch Pharm (Weinheim)* **2023**, *356* (12), 2300410. https://doi.org/10.1002/ARDP.202300410.

(36) Saraswati, A. P.; Relitti, N.; Brindisi, M.; Osko, J. D.; Chemi, G.; Federico, S.; Grillo, A.; Brogi, S.; McCabe, N. H.; Turkington, R. C.; Ibrahim, O.; O'Sullivan, J.; Lamponi, S.; Ghanim, M.; Kelly, V. P.; Zisterer, D.; Amet, R.; Hannon Barroeta, P.; Vanni, F.; Ulivieri, C.; Herp, D.; Sarno, F.; Di Costanzo, A.; Saccoccia, F.; Ruberti, G.; Jung, M.; Altucci, L.; Gemma, S.; Butini, S.; Christianson, D. W.; Campiani, G. Spiroindoline-Capped Selective HDAC6 Inhibitors: Design, Synthesis, Structural Analysis, and Biological Evaluation. *ACS Med Chem Lett* **2020**, *11* (11), 2268–2276. https://doi.org/10.1021/ACSMEDCHEMLETT.0C00395/SUPPL_FILE/ML0C00395_SI_001.PDF.

(37) Yang, W.; Wang, J.; Jiao, L.; Song, Y.; Li, C.; Hu, C. Easily Recoverable and Reusable P-Toluenesulfonic Acid for Faster Hydrolysis of Waste Polyethylene Terephthalate. *Green Chemistry* **2022**, *24* (3), 1362–1372. https://doi.org/10.1039/D1GC04567A.

(38) Federico, S.; Khan, T.; Fontana, A.; Brogi, S.; Benedetti, R.; Sarno, F.; Carullo, G.; Pezzotta, A.; Saraswati, A. P.; Passaro, E.; Pozzetti, L.; Papa, A.; Relitti, N.; Gemma, S.; Butini, S.; Pistocchi, A.; Ramunno, A.; Vincenzi, F.; Varani, K.; Tatangelo, V.; Patrussi, L.; Baldari, C. T.; Saponara, S.; Gorelli, B.; Lamponi, S.; Valoti, M.; Saccoccia, F.; Giannaccari, M.; Ruberti, G.; Herp, D.; Jung, M.; Altucci, L.; Campiani, G. Azetidin-2-One-Based Small Molecules as Dual HHDAC6/HDAC8 Inhibitors: Investigation of Their Mechanism of Action and Impact of Dual Inhibition Profile on Cell Viability. *Eur J Med Chem* **2022**, *238*, 114409. https://doi.org/10.1016/J.EJMECH.2022.114409.

(39) Porter, N. J.; Mahendran, A.; Breslow, R.; Christianson, D. W. Unusual Zinc-Binding Mode of HDAC6-Selective Hydroxamate Inhibitors. *Proc Natl Acad Sci U S A* **2017**, *114* (51), 13459–13464. https://doi.org/10.1073/PNAS.1718823114/SUPPL_FILE/PNAS.201718823SI.PDF.

(40) Shen, S.; Hadley, M.; Ustinova, K.; Pavlicek, J.; Knox, T.; Noonepalle, S.; Tavares, M. T.; Zimprich, C. A.; Zhang, G.; Robers, M. B.; Bařinka, C.; Kozikowski, A. P.; Villagra, A. Discovery of a New Isoxazole-3-Hydroxamate-Based Histone Deacetylase 6 Inhibitor SS-208 with Antitumor Activity in Syngeneic Melanoma Mouse Models. *J Med Chem* **2019**, *62* (18), 8557–8577. https://doi.org/10.1021/ACS.JMEDCHEM.9B00946/SUPPL_FILE/JM9B00946_SI_002.CSV.

(41) Bhatia, S.; Krieger, V.; Groll, M.; Osko, J. D.; Reßing, N.; Ahlert, H.; Borkhardt, A.; Kurz, T.; Christianson, D. W.; Hauer, J.; Hansen, F. K. Discovery of the First-in-Class Dual Histone Deacetylase-Proteasome Inhibitor. *J Med Chem* **2018**, *61* (22), 10299–10309. https://doi.org/10.1021/ACS.JMEDCHEM.8B01487/SUPPL_FILE/JM8B01487_SI_001.CSV.

(42) *CN114539130A - Phenyl piperazine or phenyl piperidine compound and application thereof - Google Patents*. https://patents.google.com/patent/CN114539130A/en?oq=CN114539130A (accessed 2024-05-09).

(43) *WO2023073600A1 - Compositions for preventing or treating idiopathic pulmonary fibrosis (ipf) - Google Patents*. https://patents.google.com/patent/WO2023073600A1/en?oq=WO2023073600 (accessed 2024-05-09).

(44) Pal, D.; Raj, K.; Nandi, S. S.; Sinha, S.; Mishra, A.; Mondal, A.; Lagoa, R.; Burcher, J. T.; Bishayee, A. Potential of Synthetic and Natural Compounds as Novel Histone Deacetylase Inhibitors for the Treatment of Hematological Malignancies. *Cancers 2023, Vol. 15, Page 2808* **2023**, *15* (10), 2808. https://doi.org/10.3390/CANCERS15102808.

(45) Gloghini, A.; Buglio, D.; Khaskhely, N. M.; Georgakis, G.; Orlowski, R. Z.; Neelapu, S. S.; Carbone, A.; Younes, A. Expression of Histone Deacetylases in Lymphoma: Implication for the Development of Selective Inhibitors. *Br J Haematol* **2009**, *147* (4), 515–525. https://doi.org/10.1111/J.1365-2141.2009.07887.X.

(46) Bommert, K.; Knop, S.; Arts, J.; King, P.; Page, M.; Leo, E.; Bargou, R. Novel, 2ND Generation Histone Deacetylase (HDAC) Inhibitor JNJ-26481585 Exhibits Potent Antitumor Activity Against Chronic Lymphocytic Leukemia Cells In-Vitro and Ex-Vivo. *Blood* **2007**, *110* (11), 4679. https://doi.org/10.1182/BLOOD.V110.11.4679.4679.

(47) Ninios, Y. P.; Sekeri-Pataryas, K. E.; Sourlingas, T. G. Differential Sensitivity of Human Leukemic Cell Lines to the Histone Deacetylase Inhibitor, Trichostatin A. *Leuk Res* **2010**, *34* (6), 786–792. https://doi.org/10.1016/J.LEUKRES.2009.09.004.

(48) Yang, J.; Li, D.; Zhou, J. Histone Deacetylase 6 as a Therapeutic Target in B Cell-Associated Hematological Malignancies. *Front Pharmacol* **2020**, *11*, 561318. https://doi.org/10.3389/FPHAR.2020.00971/BIBTEX.

(49) Scott, K.; Hayden, P. J.; Will, A.; Wheatley, K.; Coyne, I. Bortezomib for the Treatment of Multiple Myeloma. *Cochrane Database of Systematic Reviews* **2016**, *2016* (4). https://doi.org/10.1002/14651858.CD010816.PUB2/MEDIA/CDSR/CD010816/IMAGE_T/TCD010816-CMP-002-04.XXX.

(50) Richardson, P. G.; Zweegman, S.; O'Donnell, E. K.; Laubach, J. P.; Raje, N.; Voorhees, P.; Ferrari, R. H.; Skacel, T.; Kumar, S. K.; Lonial, S. Ixazomib for the Treatment of Multiple Myeloma. *Expert Opin Pharmacother* **2018**, *19* (17), 1949–1968. https://doi.org/10.1080/14656566.2018.1528229.

(51) Boyault, C.; Zhang, Y.; Fritah, S.; Caron, C.; Gilquin, B.; So, H. K.; Garrido, C.; Yao, T. P.; Vourc'h, C.; Matthias, P.; Khochbin, S. HDAC6 Controls Major Cell Response Pathways to Cytotoxic Accumulation of Protein Aggregates. *Genes Dev* **2007**, *21* (17), 2172–2181. https://doi.org/10.1101/GAD.436407.

(52) Lee, D. H.; Kim, G. W.; Kwon, S. H. The HDAC6-Selective Inhibitor Is Effective against Non-Hodgkin Lymphoma and Synergizes with Ibrutinib in Follicular Lymphoma. *Mol Carcinog* **2019**, *58* (6), 944–956. https://doi.org/10.1002/MC.22983.

(53) Ren, J.; Catalina, M. D.; Eden, K.; Liao, X.; Read, K. A.; Luo, X.; McMillan, R. P.; Hulver, M. W.; Jarpe, M.; Bachali, P.; Grammer, A. C.; Lipsky, P. E.; Reilly, C. M. Selective Histone Deacetylase 6 Inhibition Normalizes B Cell Activation and Germinal Center Formation in a Model of Systemic Lupus Erythematosus. *Front Immunol* **2019**, *10* (OCT). https://doi.org/10.3389/FIMMU.2019.02512.

(54) Campiani, G.; Khan, T.; Ulivieri, C.; Staiano, L.; Papulino, C.; Magnano, S.; Nathwani, S.; Ramunno, A.; Lucena-Agell, D.; Relitti, N.; Federico, S.; Pozzetti, L.; Carullo, G.; Casagni, A.; Brogi, S.; Vanni, F.; Galatello, P.; Ghanim, M.; McCabe, N.; Lamponi, S.; Valoti, M.; Ibrahim, O.; O'Sullivan, J.; Turkington, R.; Kelly, V. P.; VanWemmel, R.; Díaz, J. F.; Gemma, S.; Zisterer, D.; Altucci, L.; De Matteis, A.; Butini, S.; Benedetti, R. Design and Synthesis of Multifunctional Microtubule Targeting Agents Endowed with Dual Pro-Apoptotic and Anti-Autophagic Efficacy. *Eur J Med Chem* **2022**, *235*, 114274. https://doi.org/10.1016/J.EJMECH.2022.114274.

(55) Carullo, G.; Bottoni, L.; Pasquini, S.; Papa, A.; Contri, C.; Brogi, S.; Calderone, V.; Orlandini, M.; Gemma, S.; Varani, K.; Butini, S.; Galvagni, F.; Vincenzi, F.; Campiani, G. Synthesis of Unsymmetrical Squaramides as Allosteric GSK-3β Inhibitors Promoting β-Catenin-Mediated Transcription of TCF/LEF in Retinal Pigment Epithelial Cells. *ChemMedChem* **2022**, *17* (24). https://doi.org/10.1002/CMDC.202200456.

(56) Lin, H. F.; Traver, D.; Zhu, H.; Dooley, K.; Paw, B. H.; Zon, L. I.; Handin, R. I. Analysis of Thrombocyte Development in CD41-GFP Transgenic Zebrafish. *Blood* **2005**, *106* (12), 3803–3810. https://doi.org/10.1182/BLOOD-2005-01-0179.

(57) Davidson, A. J.; Zon, L. I. The 'Definitive' (and 'Primitive') Guide to Zebrafish Hematopoiesis. *Oncogene 2004 23:43* **2004**, *23* (43), 7233–7246. https://doi.org/10.1038/sj.onc.1207943.

(58) Dumas, P. Y.; Raffoux, E.; Bérard, E.; Bertoli, S.; Hospital, M. A.; Heiblig, M.; Desbrosses, Y.; Bonmati, C.; Pautas, C.; Lambert, J.; Orvain, C.; Banos, A.; Pasquier, F.; Peterlin, P.; Marchand, T.; Uzunov, M.; Frayfer, J.; Turlure, P.; Cluzeau, T.; Jourdan, E.; Himberlin, C.; Tavernier, E.; Villate, A.; Haiat, S.; Chretien, M. L.; Carre, M.; Chantepie, S.; Vaida, I.; Wemeau, M.; Chebrek, S.; Guillerm, G.; Guièze, R.; Debarri, H.; Gehlkopf, E.; Laribi, K.; Marcais, A.; Santagostino, A.; Béné, M. C.; Mineur, A.; Pigneux, A.; Dombret, H.; Récher, C. Gilteritinib Activity in Refractory or Relapsed FLT3-Mutated Acute Myeloid

Leukemia Patients Previously Treated by Intensive Chemotherapy and Midostaurin: A Study from the French AML Intergroup ALFA/FILO. *Leukemia 2022 37:1* **2022**, *37* (1), 91–101. https://doi.org/10.1038/s41375-022-01742-7.

(59) Pezzotta, A.; Brioschi, L.; Carbone, S.; Mazzoleni, B.; Bontempi, V.; Monastra, F.; Mauri, L.; Marozzi, A.; Mione, M.; Pistocchi, A.; Viani, P. Combined Inhibition of Hedgehog and HDAC6: In Vitro and In Vivo Studies Reveal a New Role for Lysosomal Stress in Reducing Glioblastoma Cell Viability. *Int J Mol Sci* **2023**, *24* (6), 5771. https://doi.org/10.3390/IJMS24065771/S1.

(60) Vallone, A.; D'Alessandro, S.; Brogi, S.; Brindisi, M.; Chemi, G.; Alfano, G.; Lamponi, S.; Lee, S. G.; Jez, J. M.; Koolen, K. J. M.; Dechering, K. J.; Saponara, S.; Fusi, F.; Gorelli, B.; Taramelli, D.; Parapini, S.; Caldelari, R.; Campiani, G.; Gemma, S.; Butini, S. Antimalarial Agents against Both Sexual and Asexual Parasites Stages: Structure-Activity Relationships and Biological Studies of the Malaria Box Compound 1-[5-(4-Bromo-2-Chlorophenyl)Furan-2-Yl]-N-[(Piperidin-4-Yl)Methyl]Methanamine (MMV019918) and Analog. *Eur J Med Chem* **2018**, *150*, 698–718. https://doi.org/https://doi.org/10.1016/j.ejmech.2018.03.024.

(61) Carullo, G.; Saponara, S.; Ahmed, A.; Gorelli, B.; Mazzotta, S.; Trezza, A.; Gianibbi, B.; Campiani, G.; Fusi, F.; Aiello, F. Novel Labdane Diterpenes-Based Synthetic Derivatives: Identification of a Bifunctional Vasodilator That Inhibits CaV1.2 and Stimulates KCa1.1 Channels. *Mar Drugs* **2022**, *20* (8), 515. https://doi.org/10.3390/md20080515.

(62) Carullo, G.; Borghini, F.; Fusi, F.; Saponara, S.; Fontana, A.; Pozzetti, L.; Fedeli, R.; Panti, A.; Gorelli, B.; Aquino, G.; Basilicata, M. G.; Pepe, G.; Campiglia, P.; Biagiotti, S.; Gemma, S.; Butini, S.; Pianezze, S.; Loppi, S.; Cavaglioni, A.; Perini, M.; Campiani, G. Traceability and Authentication in Agri-Food Production: A Multivariate Approach to the Characterization of the Italian Food Excellence Elephant Garlic (Allium Ampeloprasum L.), a Vasoactive Nutraceutical. *Food Chem* **2024**, *444*, 138684. https://doi.org/10.1016/J.FOODCHEM.2024.138684.

(63) Protein Preparation Wizard, Schrödinger, LLC, New York, NY, 2021,.

(64) Lu, C.; Wu, C.; Ghoreishi, D.; Chen, W.; Wang, L.; Damm, W.; Ross, G. A.; Dahlgren, M. K.; Russell, E.; Von Bargen, C. D.; Abel, R.; Friesner, R. A.; Harder, E. D. OPLS4: Improving Force Field Accuracy on Challenging Regimes of Chemical Space. *J Chem Theory Comput* **2021**, *17* (7), 4291–4300. https://doi.org/10.1021/acs.jctc.1c00302.

(65) Glide, Version 9.1; Schrödinger, LLC: New York, 2021.

(66) *Life Science: LigPrep - Schrödinger*. https://newsite.schrodinger.com/platform/products/ligprep/ (accessed 2024-03-02).

(67) *Life Science: MacroModel - Schrödinger*. https://newsite.schrodinger.com/platform/products/macromodel/ (accessed 2024-03-02).

(68) Clark Still, W.; Tempczyk, A.; Hawley, R. C.; Hendrickson, T. Semianalytical Treatment of Solvation for Molecular Mechanics and Dynamics. *J Am Chem Soc* **1990**, *112* (16), 6127–6129. https://doi.org/10.1021/JA00172A038/SUPPL_FILE/JA00172A038_SI_001.PDF.

(69) Polak, E.; Ribiere, G. Note Sur La Convergence de Méthodes de Directions Conjuguées. *Revue française d'informatique et de recherche opérationnelle. Série rouge* **1969**, *3* (R1), 35–43.

(70) Kimmel, C. B.; Ballard, W. W.; Kimmel, S. R.; Ullmann, B.; Schilling, T. F. Stages of Embryonic Development of the Zebrafish. *Developmental Dynamics* **1995**, *203* (3), 253–310. https://doi.org/10.1002/AJA.1002030302.

(71) Thisse, C.; Thisse, B. High-Resolution in Situ Hybridization to Whole-Mount Zebrafish Embryos. *Nature Protocols 2008 3:1* **2007**, *3* (1), 59–69. https://doi.org/10.1038/nprot.2007.514.

(72) Dobrzycki, T.; Krecsmarik, M.; Monteiro, R. Genotyping and Quantification of In Situ Hybridization Staining in Zebrafish. *J Vis Exp* **2020**, *2020* (155). https://doi.org/10.3791/59956.

(73) Pessina, F.; Gamberucci, A.; Chen, J.; Liu, B.; Vangheluwe, P.; Gorelli, B.; Lorenzini, S.; Spiga, O.; Trezza, A.; Sgaragli, G.; Saponara, S. Negative Chronotropism, Positive Inotropism and Lusitropism of 3,5-Di-t-Butyl-4-Hydroxyanisole (DTBHA) on Rat Heart Preparations Occur through Reduction of RyR2 Ca(2+) Leak. *Biochem Pharmacol* **2018**, *155*, 434–443. https://doi.org/10.1016/j.bcp.2018.07.026.

(74) Ferrara, A.; Fusi, F.; Gorelli, B.; Sgaragli, G.; Saponara, S. Effects of Freeze-Dried Red Wine on Cardiac Function and ECG of the Langendorff-Perfused Rat Heart. *Can J Physiol Pharmacol* **2014**, *92* (2), 171–174. https://doi.org/10.1139/cjpp-2013-0262.

(75) Papa, A.; Pasquini, S.; Galvani, F.; Cammarota, M.; Contri, C.; Carullo, G.; Gemma, S.; Ramunno, A.; Lamponi, S.; Gorelli, B.; Saponara, S.; Varani, K.; Mor, M.; Campiani, G.; Boscia, F.; Vincenzi, F.; Lodola, A.; Butini, S. Development of Potent and Selective FAAH Inhibitors with Improved Drug-like Properties as Potential Tools to Treat Neuroinflammatory Conditions. *Eur J Med Chem* **2023**, *246*, 114952. https://doi.org/10.1016/J.EJMECH.2022.114952.

(76) Fusi, F.; Durante, M.; Gorelli, B.; Perrone, M. G.; Colabufo, N. A.; Saponara, S. MC225, a Novel Probe for P-Glycoprotein PET Imaging at the Blood–Brain Barrier: In Vitro Cardiovascular Safety Evaluation. *J Cardiovasc Pharmacol* **2017**, *70* (6).

Supporting Information
The Supporting Information is available free of charge at XXXXX

Chemistry Section: synthesis and characterization of compounds **5a-q**
Biological Section: cell viability, target engagement, apoptotic profile, *in vivo* studies
Figure S1. Effect of the novel HDACis on HEK-293 cell viability.
Figure S2. Cell viability assay in MM.1S, BONNA-12 and PBMCs.
Table S1. Evaluation of the physicochemical properties of selected compounds **5c**, **5g**, **5h**, **5k** and TUB.
Figure S3. Morphological assays in **5c**, **5g** and **5h** treated embryos
Figure S4. Survival and morphological analysis of **5c**, **5g** and **5h** treated embryos.
Figure S5. Effects of **5c** on LVP and CPP in Langendorff-perfused rat hearts.
Table S2. Effects of **5c** on HR, RR, PQ, QRS, QT, and QTc in Langendorff Perfused Rat Hearts
^{1}H NMR spectra of compounds **5a-e**, **5g-p**

For Table of Contents Use Only

Development of Epigenetic Modifiers with Therapeutic Potential in Fms-related tyrosine Kinase 3 / Internal Tandem Duplication (FLT3/ITD) Acute Myeloid Leukemia and other Blood Malignancies

Gabriele Carullo[1,#], Sara Rossi[1,#], Valentina Giudice[2], Alex Pezzotta[3], Ugo Chianese[4], Pasqualina Scala[2], Sabrina Carbone[3], Anna Fontana[1], Giovanna Panzeca[1], Silvia Pasquini[5], Chiara Contri[6], Sandra Gemma[1,*], Anna Ramunno[7], Simona Saponara[8], Francesca Galvani[9], Alessio Lodola[9], Marco Mor[9], Rosaria Benedetti[4,10], Carmine Selleri[2], Katia Varani[6], Stefania Butini[1], Lucia Altucci[4,10,11], Fabrizio Vincenzi[6], Anna Pistocchi[3], Giuseppe Campiani[1,12,*]

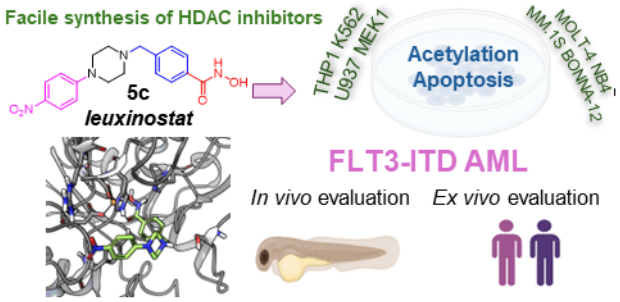

Synopsis

New HDAC inhibitors have been prepared and tested in different blood cancer cells, including chronic and acute leukemias. **5c** (*leuxinostat*) was identified as a promising tool for the treatment of FLT3/ITD AML, with *in vivo* and *ex vivo* efficacy.